

# ENV-167

# Aerosol measurement technologies

Satoshi Takahama

Laboratory for Environmental Spectrochemistry

17.11.2025

# About me

## Formation

- BS Civil Engineering
- PhD Chemical Engineering
- Scripps Institution of Oceanography
- EPFL

Research in aerosol science, air pollution monitoring, and atmospheric chemistry

Teaching Computational Methods and Tools (BA3) and Air Pollution (MA2)

# After this lecture, you will be able to answer the following questions

- Why do we care about atmospheric aerosols?
- What are some properties of atmospheric aerosols?
- Why do we need to measure chemical constituents?
- What are important light-matter interactions?
- What are the impediments to ubiquitous chemical measurements?

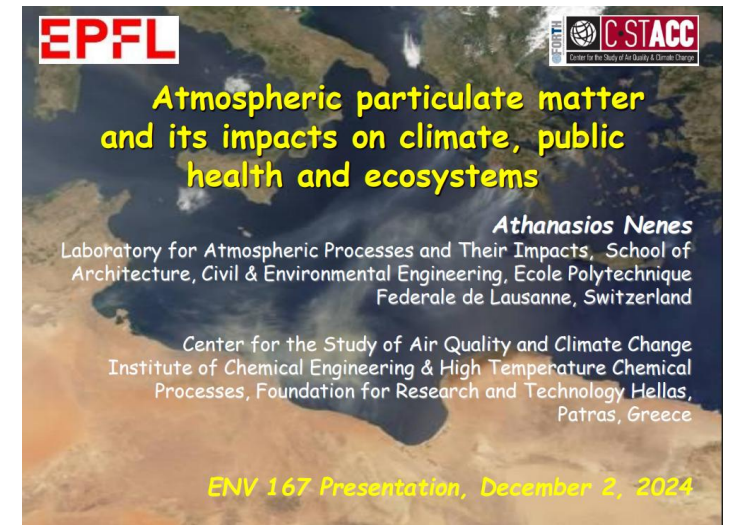
Related lectures:

# Outline

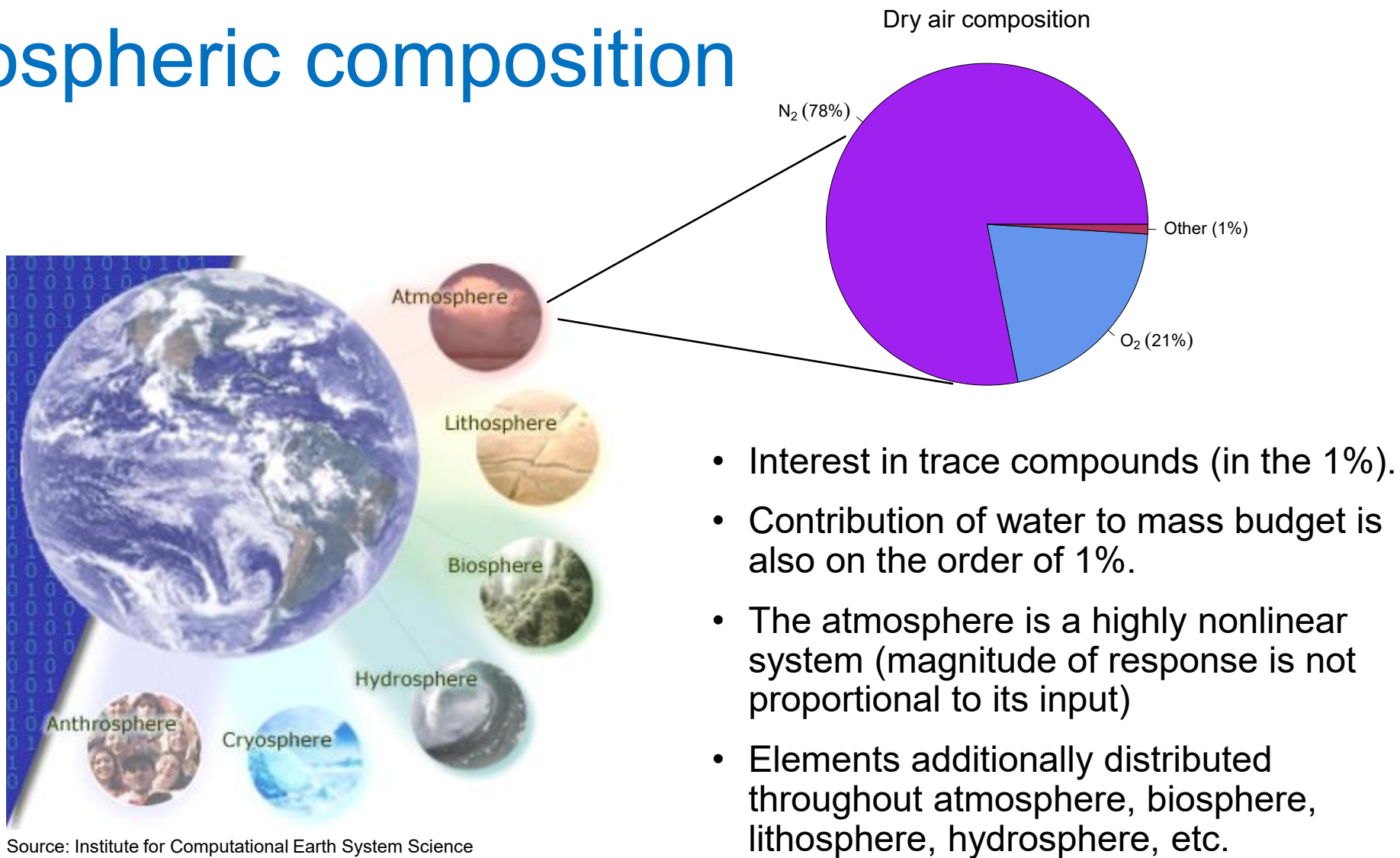
- Atmospheric composition
- Aerosols
- Aerosol impacts on climate and health
- Light-matter interactions
- Environmental monitoring via infrared

“To reduce pollution, you must first measure it”

“You can’t improve what you don’t measure”



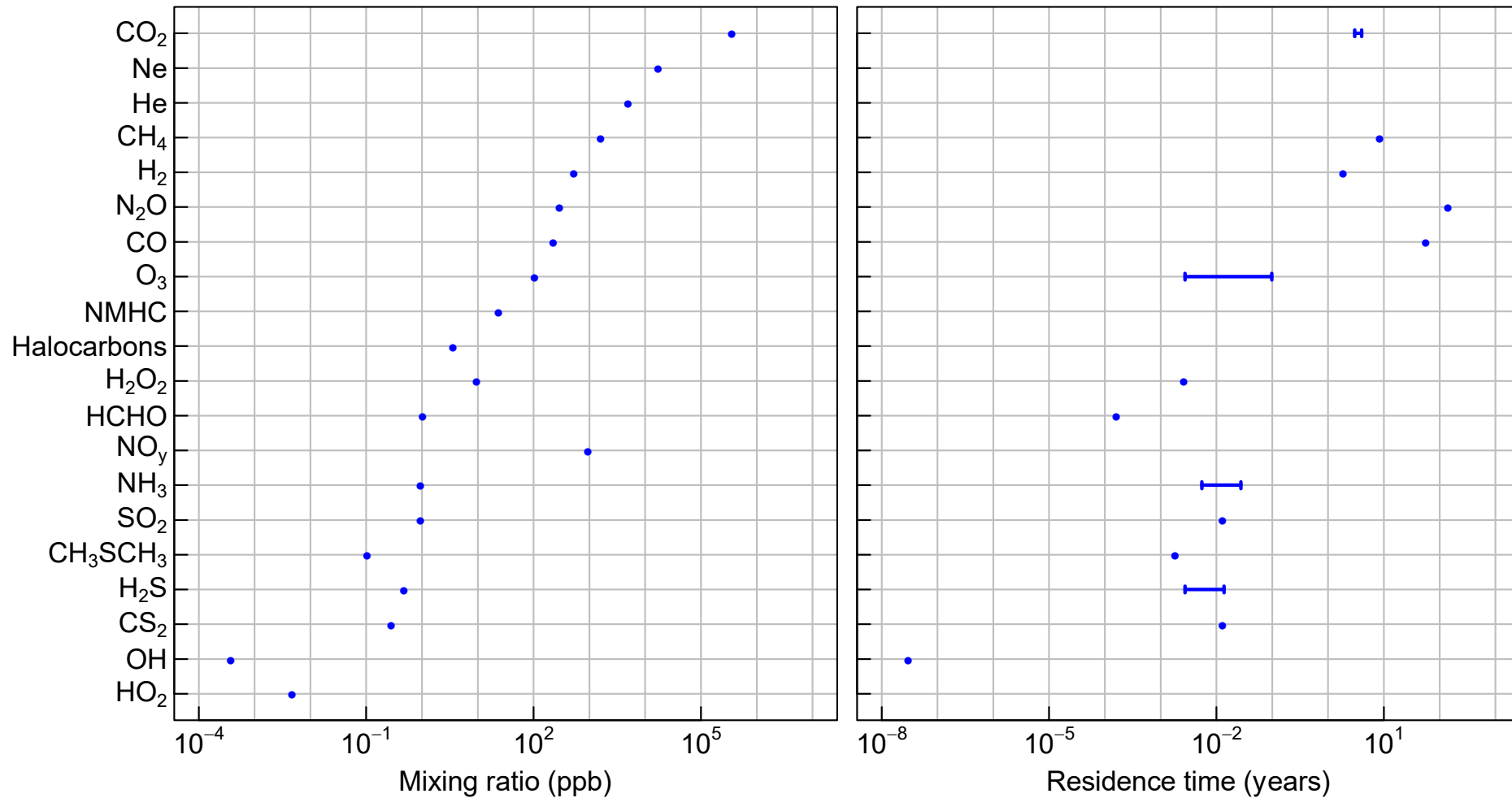
# Atmospheric composition



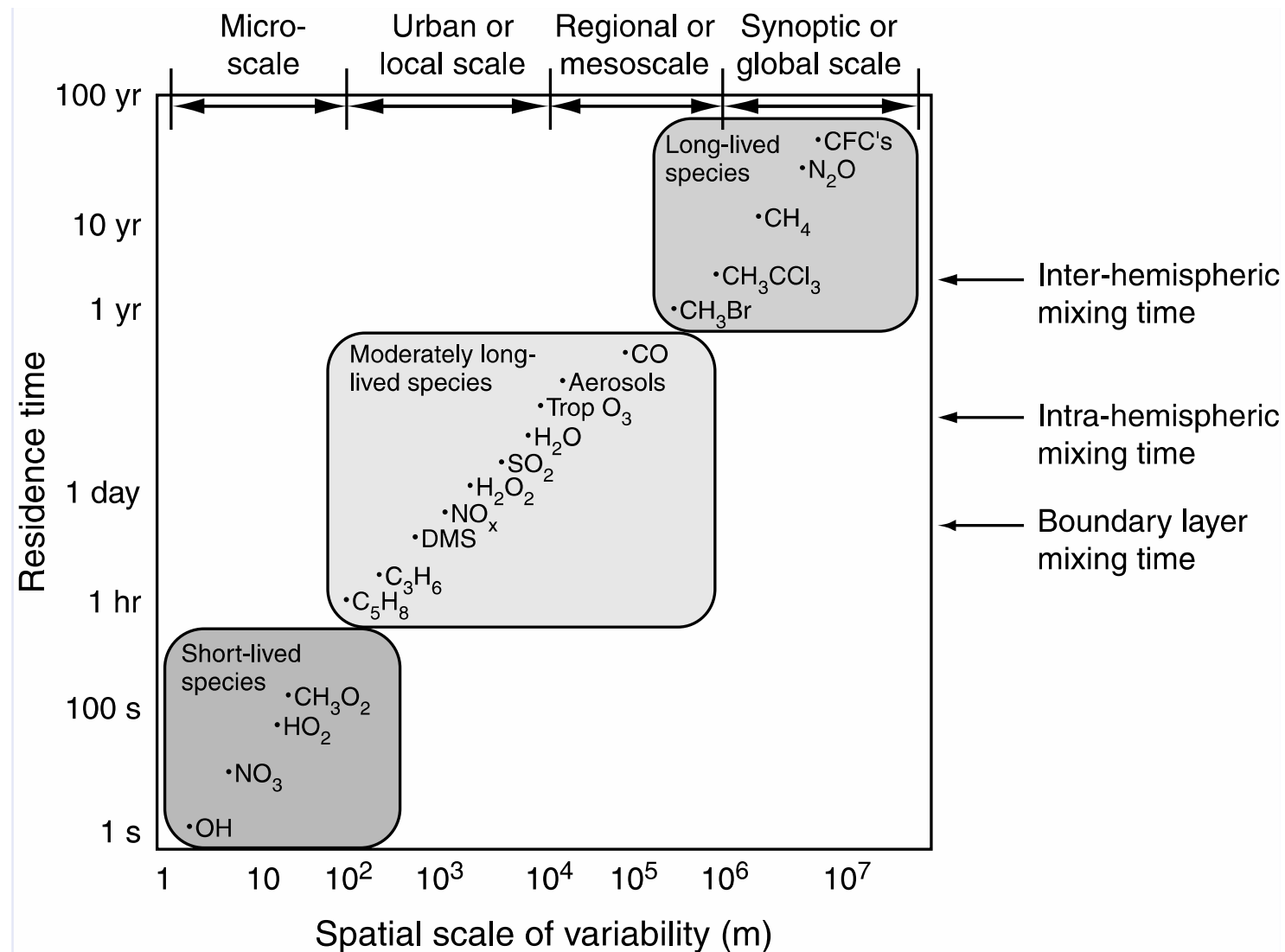
Source: Institute for Computational Earth System Science

# Tropospheric species in the gas phase

Data from Wallace and Hobbs, 2006



# Residence Time and Spatial Scales of Variation of Chemicals in the Atmosphere



### Feinstaub (PM2.5): Jahresmittel 2022

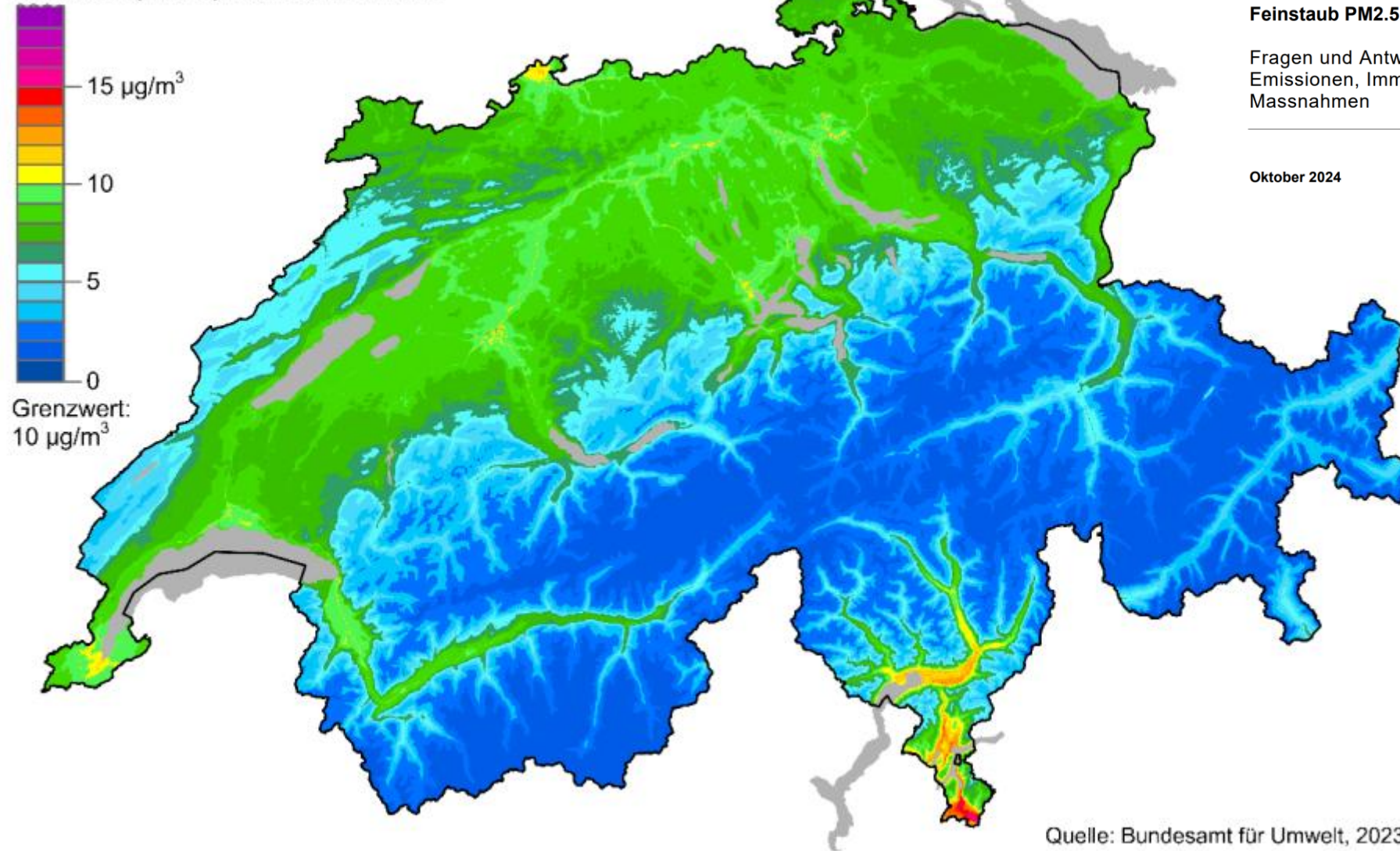
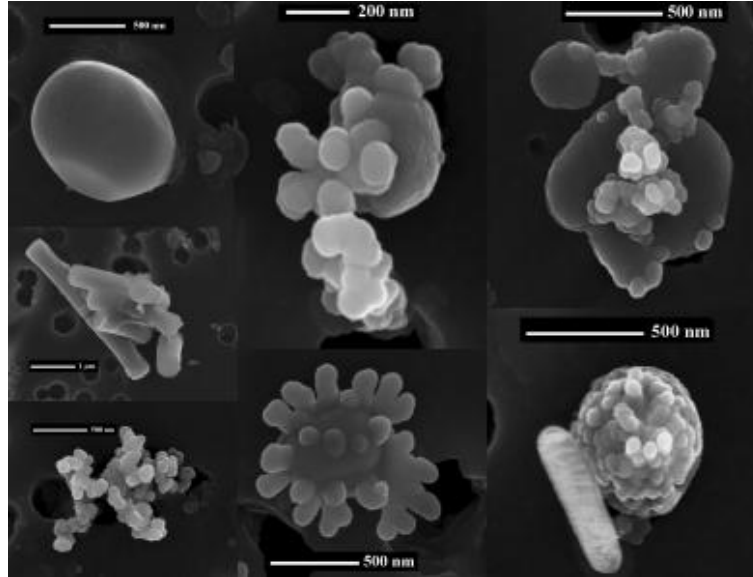


**Abbildung 4** Jahresmittel 2022 von PM2.5, berechnet aus einer Kombination von Messwerten und Modelldaten.

# Atmospheric aerosols

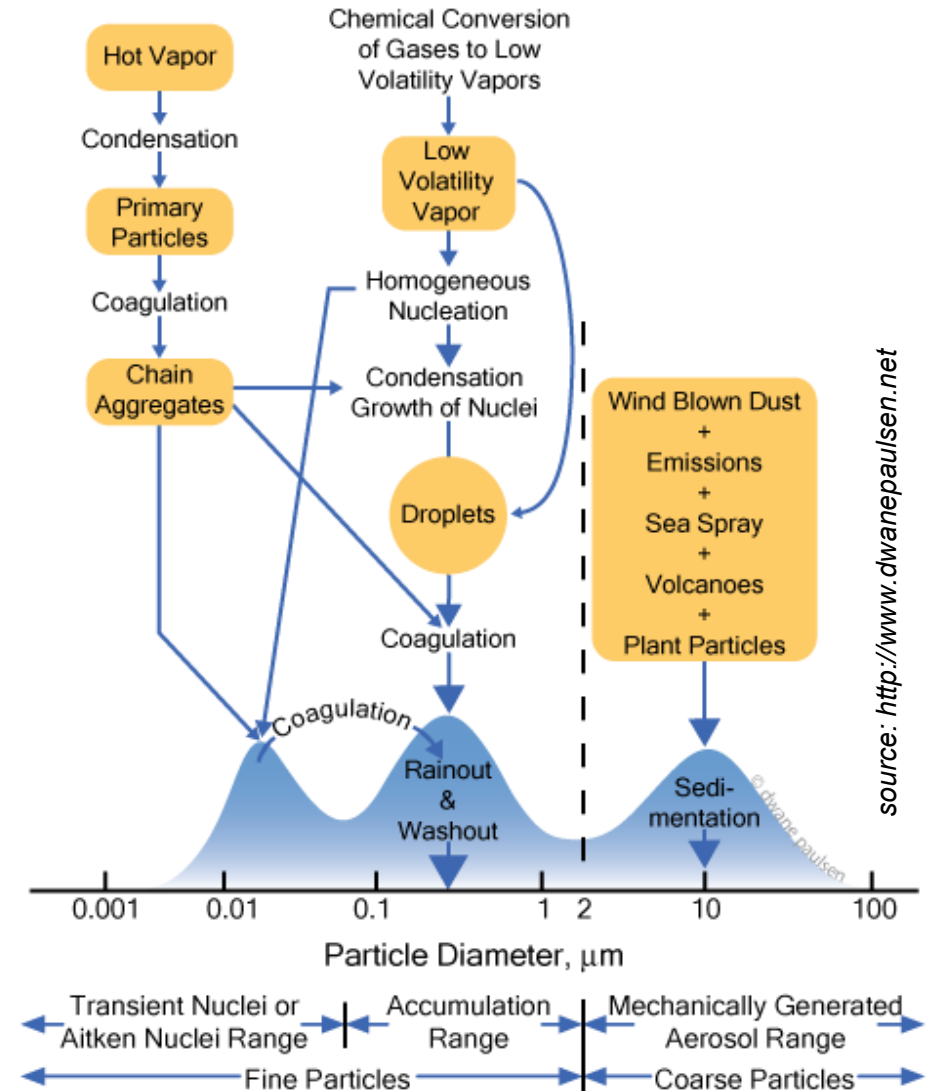
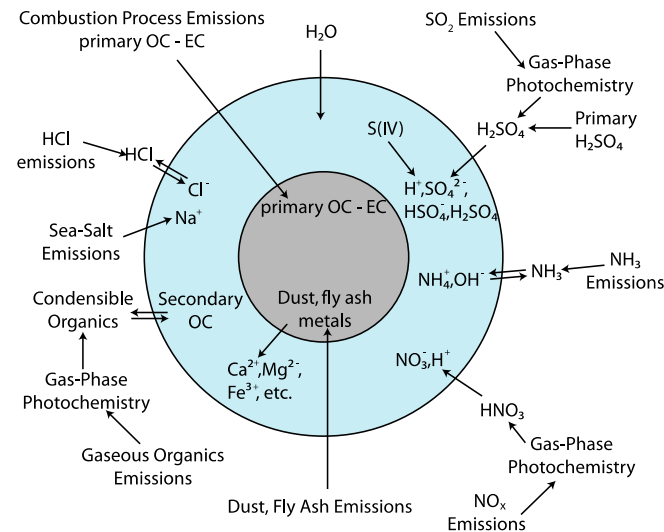
## Scanning electron microscopy images



Coz et al., *Aerosol Sci. Tech.*, 2008

- Varies in
- size
  - shape
  - phase
  - composition

adapted from Pandis et al.,  
*J. Phys. Chem.*, 1995



source: <http://www.dwanepaulsen.net>

# Aerosol sources

Mixed



Forest fires



Sea spray



Dust

Natural



Volcanic eruptions



Traffic / Transport



Domestic activities



Industry



Agriculture

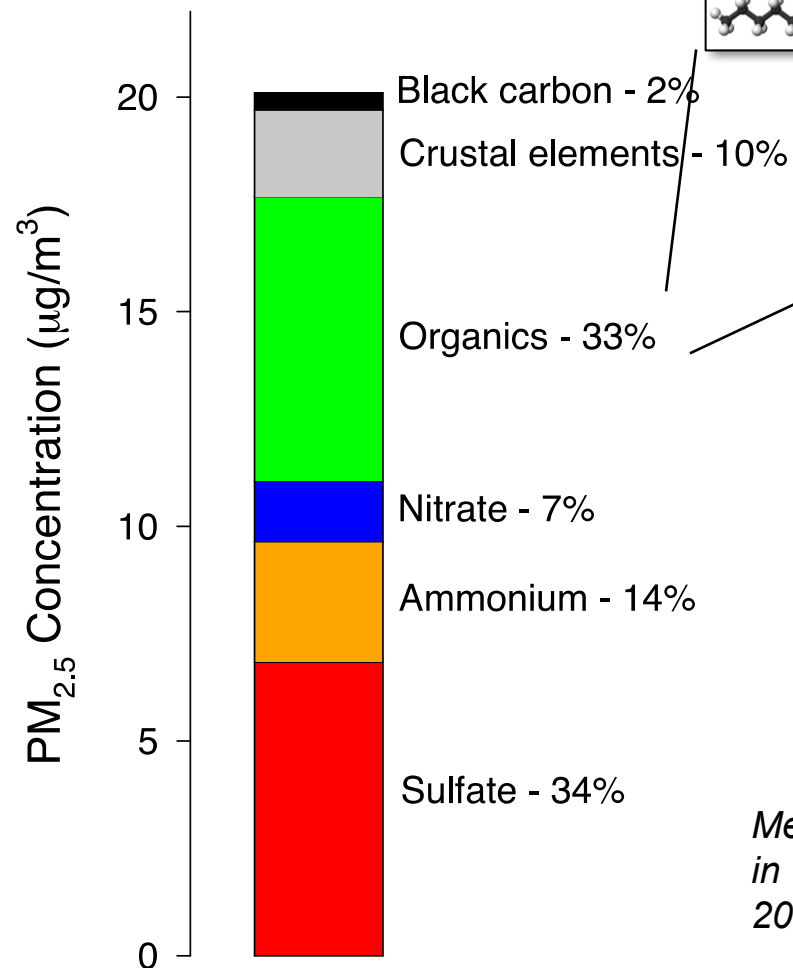
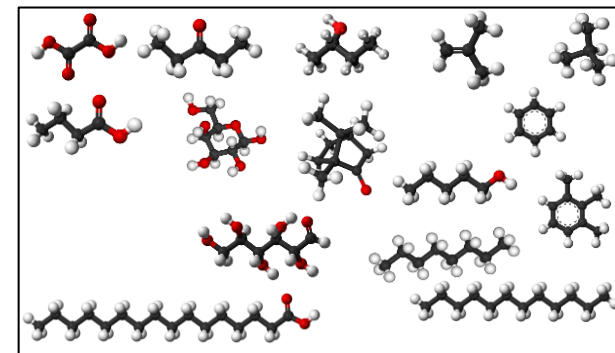
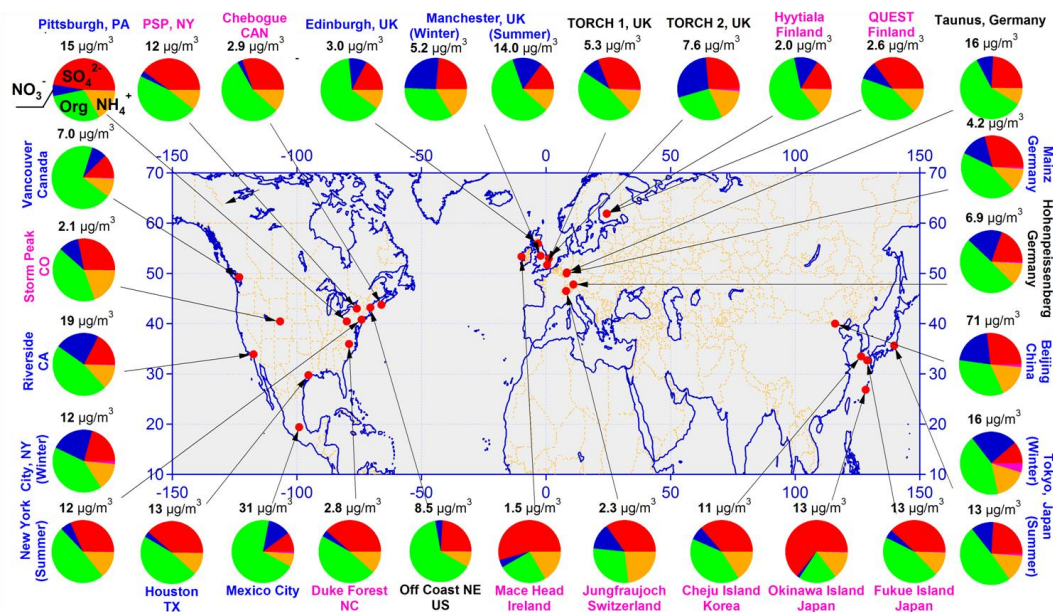
Anthropogenic

# Aerosol composition

## Major components:

- Inorganic salts/ions
- Organic compounds (10,000+)
- Black carbon/soot
- Mineral dust

Occurs in different proportions over time and throughout the world

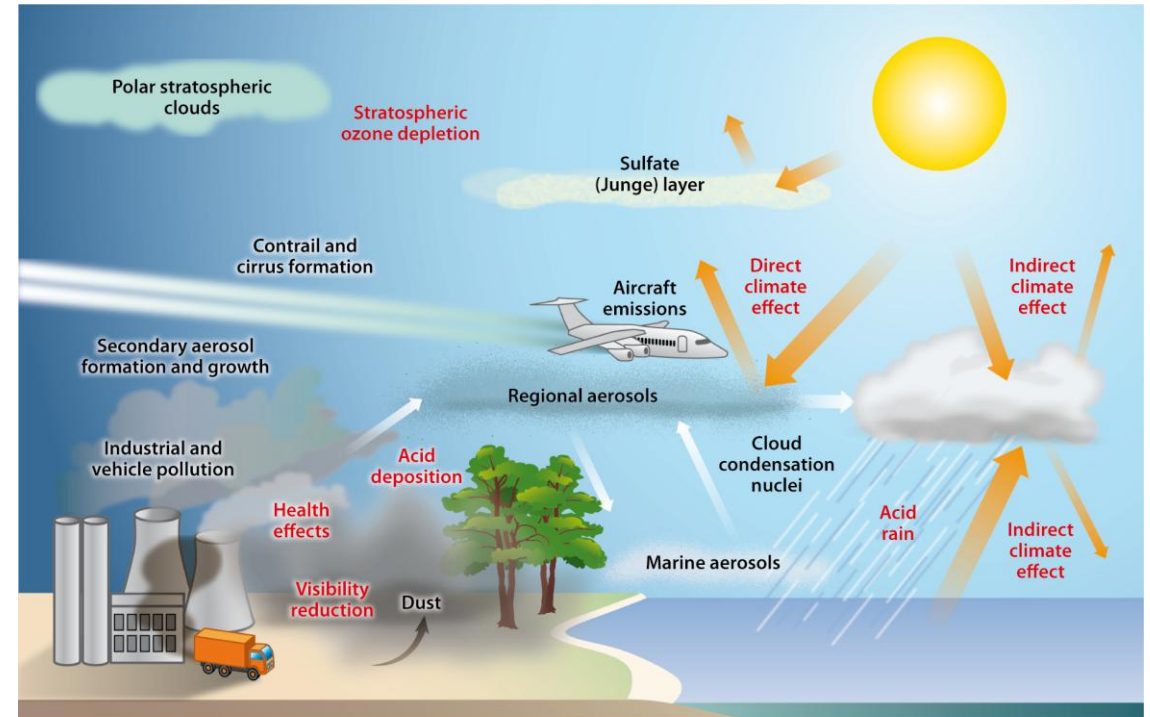
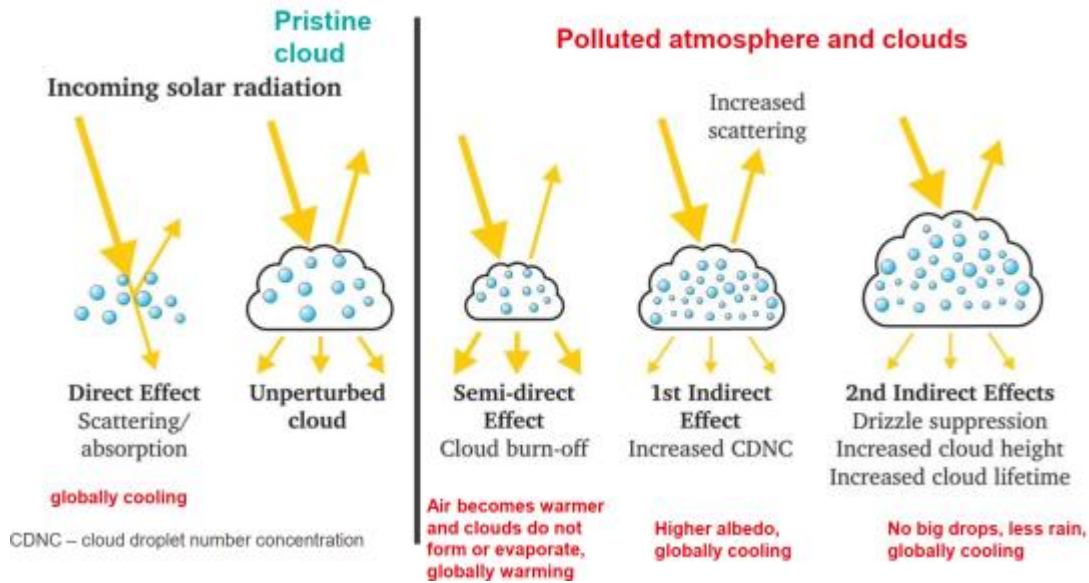
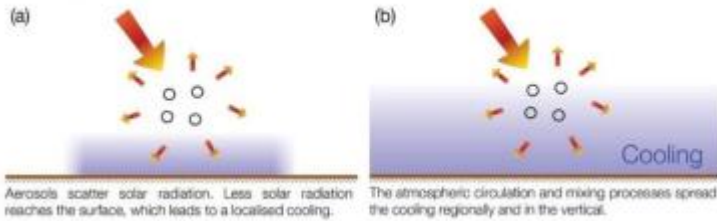


Pittsburgh, PA 2001

Mean composition  
in Western Pennsylvania, USA  
2001

# Aerosols and climate

## Scattering aerosols

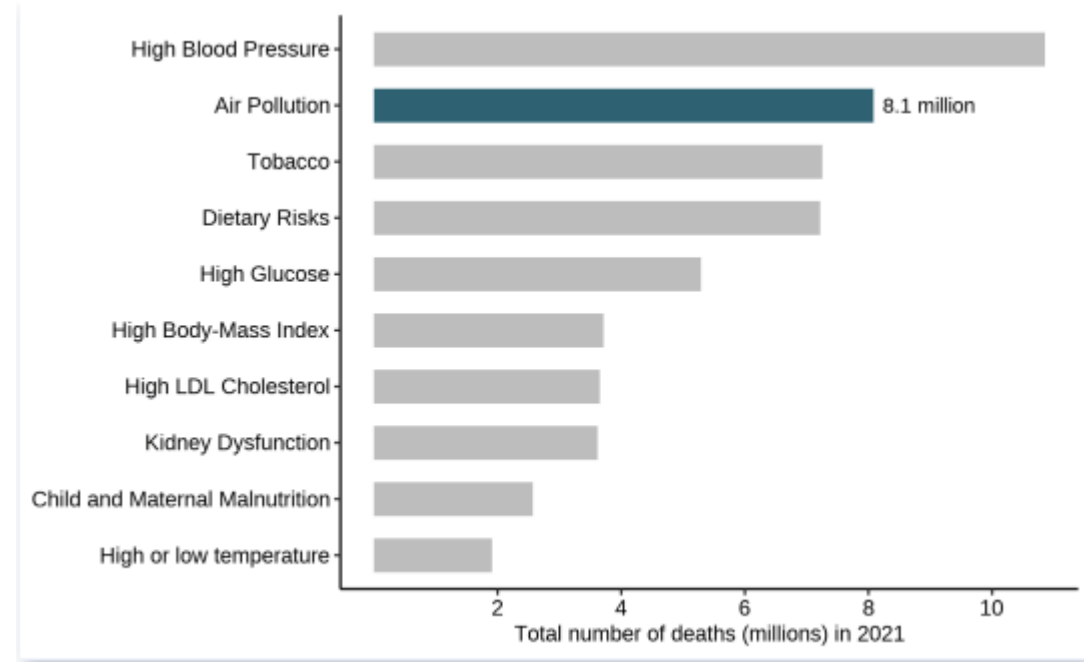


**AR** Kolb CE, Worsnop DR. 2012. Annu. Rev. Phys. Chem. 63:471–91

# Aerosols and health

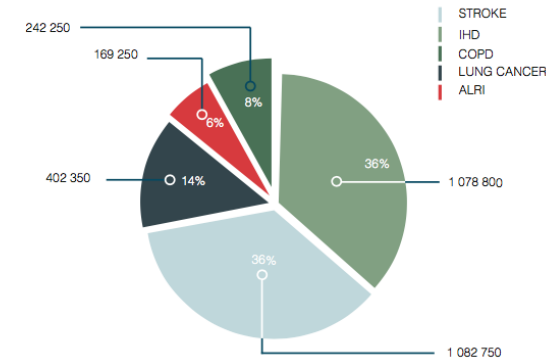
# Particulate matter and health

- Mortality
- Respiratory illnesses
- Cardiovascular effects
- Neurodegenerative diseases



<https://vizhub.healthdata.org/gbd-compare/>  
*State of Global Air 2024*

Figure 20: Deaths attributable to AAP in 2012, by disease



Percentage represents percentage of total AAP burden. AAP: ambient air pollution; ALRI: acute lower respiratory disease; COPD: chronic obstructive pulmonary disease; IHD: ischaemic heart disease.

source: WHO

# The New England Journal of Medicine

©Copyright, 1993, by the Massachusetts Medical Society

Volume 329

DECEMBER 9, 1993

Number 24

## AN ASSOCIATION BETWEEN AIR POLLUTION AND MORTALITY IN SIX U.S. CITIES

DOUGLAS W. DOCKERY, SC.D., C. ARDEN POPE III, PH.D., XIPING XU, M.D., PH.D.,  
JOHN D. SPENGLER, PH.D., JAMES H. WARE, PH.D., MARTHA E. FAY, M.P.H.,  
BENJAMIN G. FERRIS, JR., M.D., AND FRANK E. SPEIZER, M.D.

### Cohort study of 8111 Americans

Medical history and lifestyle examined over 14-16 years

Association found between excess mortality and fine particulate matter pollution

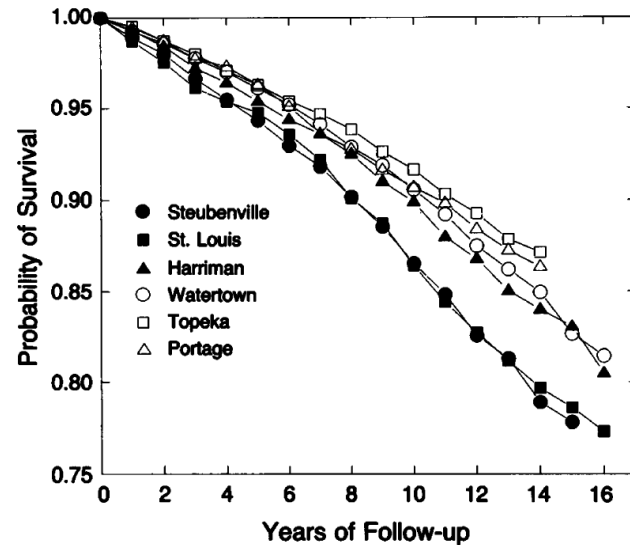


Figure 2. Crude Probability of Survival in the Six Cities, According to Years of Follow-up.

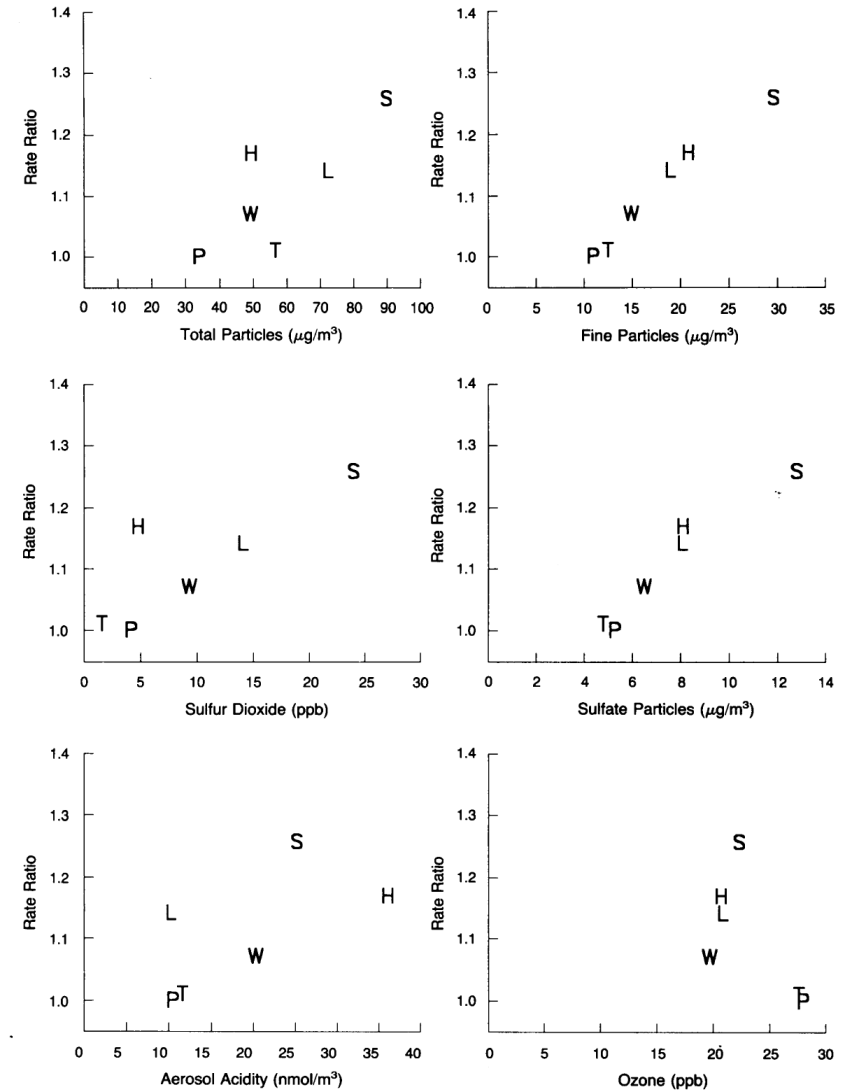


Figure 3. Estimated Adjusted Mortality-Rate Ratios and Pollution Levels in the Six Cities. The cities are shown for the measures of air pollution. P denotes Portage, Wisconsin; T Topeka, Kansas; W Watertown, Massachusetts; L St. Louis; H Harriman, Tennessee; and S Steubenville, Ohio.

# Survival analysis

## Cox proportional hazards model

$$\lambda_A(t) = -\frac{d}{dt} \ln S(t)$$

↑  
survival probability

Incidence rate

Baseline incidence rate

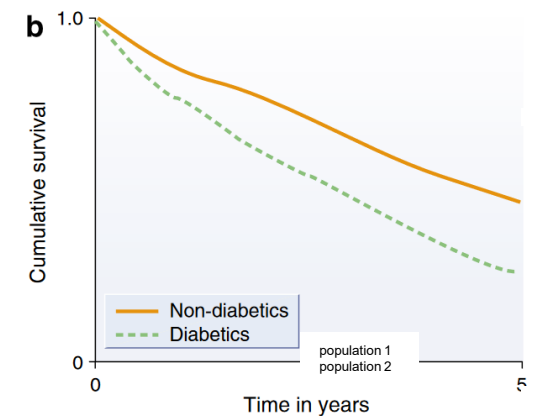
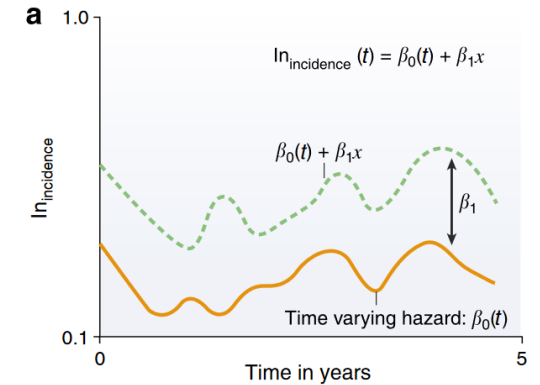
Confounders

Exposure

$$\lambda_A(t) = \lambda_B(t) \times \exp \left( \sum_{i=1}^k \beta_i X_i + \gamma E \right)$$

Log-linear relation to exposure

$$\ln \lambda_A(t) = \beta_0(t) + \sum_{i=1}^k \beta_i X_i + \gamma E$$



adapted from van Dijk et al., 2008

# Confounders

- Stratified by age group and sex
- Smoking
- Education level
- BMI
- Exposure to local sources (occupational exposure)

# Improvements in estimates (1993 – present)

- Larger cohorts
- Better exposure estimate
  - combine ground-based measurements, satellite remote sensing, and air quality model simulations
  - high resolution
  - capture microenvironments
- More confounding variables
  - environmental variables
  - behavioral, social, and economic variables
  - demographic variables
- Specific chemical constituents

# Global urban temporal trends in fine particulate matter (PM<sub>2.5</sub>) and attributable health burdens: estimates from global datasets

Veronica A Southerland, Michael Brauer, Arash Mohegh, Melanie S Hammer, Aaron van Donkelaar, Randall V Martin, Joshua S Apte, Susan C Anenberg

Lancet Planet Health 2022;  
6: e139–46

Published Online

January 5, 2022

[https://doi.org/10.1016/](https://doi.org/10.1016/S2542-5196(21)00350-8)

S2542-5196(21)00350-8

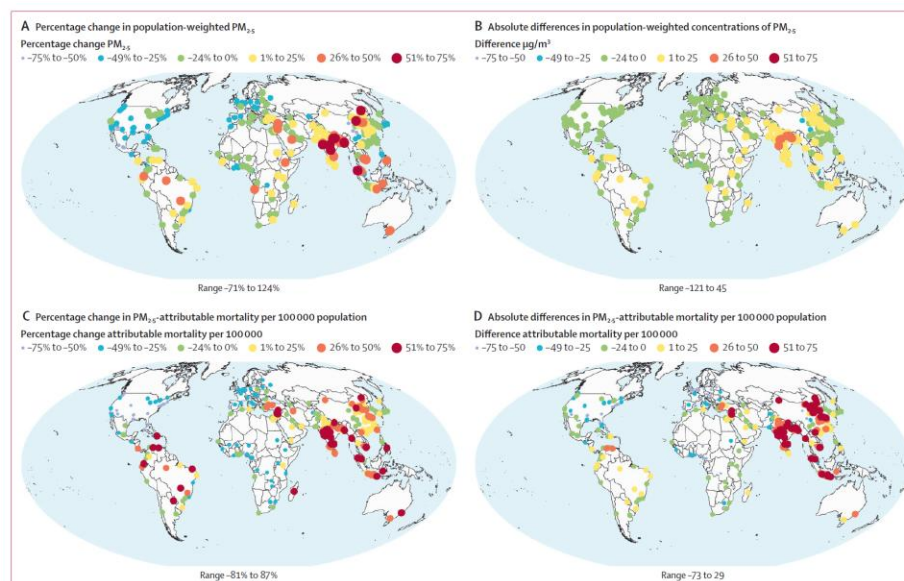


Figure 3: Change in population-weighted PM<sub>2.5</sub> concentrations and PM<sub>2.5</sub>-attributable mortality rates between 2000 and 2019 for the top 250 most populated urban areas based on 2019 WorldPop estimates  
(A) Percentage change in population-weighted PM<sub>2.5</sub> concentrations. (B) Absolute differences in population-weighted concentrations of PM<sub>2.5</sub>. (C) Percentage change in PM<sub>2.5</sub>-attributable mortality per 100 000 population. (D) Absolute differences in PM<sub>2.5</sub>-attributable mortality per 100 000 population.

## Summary

**Background** With much of the world's population residing in urban areas, an understanding of air pollution exposures at the city level can inform mitigation approaches. Previous studies of global urban air pollution have not considered trends in air pollutant concentrations nor corresponding attributable mortality burdens. We aimed to estimate trends in fine particulate matter (PM<sub>2.5</sub>) concentrations and associated mortality for cities globally.

**Methods** We use high-resolution annual average PM<sub>2.5</sub> concentrations, epidemiologically derived concentration response functions, and country-level baseline disease rates to estimate population-weighted PM<sub>2.5</sub> concentrations and attributable cause-specific mortality in 13 160 urban centres between the years 2000 and 2019.

**Findings** Although regional averages of urban PM<sub>2.5</sub> concentrations decreased between the years 2000 and 2019, we found considerable heterogeneity in trends of PM<sub>2.5</sub> concentrations between urban areas. Approximately 86% (2.5 billion inhabitants) of urban inhabitants lived in urban areas that exceeded WHO's 2005 guideline annual average PM<sub>2.5</sub> (10 µg/m<sup>3</sup>), resulting in an excess of 1.8 million (95% CI 1.34 million–2.3 million) deaths in 2019. Regional averages of PM<sub>2.5</sub>-attributable deaths increased in all regions except for Europe and the Americas, driven by changes in population numbers, age structures, and disease rates. In some cities, PM<sub>2.5</sub>-attributable mortality increased despite decreases in PM<sub>2.5</sub> concentrations, resulting from shifting age distributions and rates of non-communicable disease.

**Interpretation** Our study showed that, between the years 2000 and 2019, most of the world's urban population lived in areas with unhealthy levels of PM<sub>2.5</sub>, leading to substantial contributions to non-communicable disease burdens. Our results highlight that avoiding the large public health burden from urban PM<sub>2.5</sub> will require strategies that reduce exposure through emissions mitigation, as well as strategies that reduce vulnerability to PM<sub>2.5</sub> by improving overall public health.

A pollutant is a substance detectable in the environment, at least partially due to human activity, and that may induce adverse effects on the living organisms.

Moriarty 1983

(Breider lecture)



Guideline levels for each pollutant ( $\mu\text{g}/\text{m}^3$ ):		
PM <sub>2.5</sub>	1 year	<del>10</del>
	24 h (99th percentile)	25
PM <sub>10</sub>	1 year	20
	24 h (99th percentile)	50
Ozone, O <sub>3</sub>	8 h, daily maximum	100
Nitrogen dioxide, NO <sub>2</sub>	1 yr	40
	1 h	200
Sulfur dioxide, SO <sub>2</sub>	24 h	20
	10 min	500

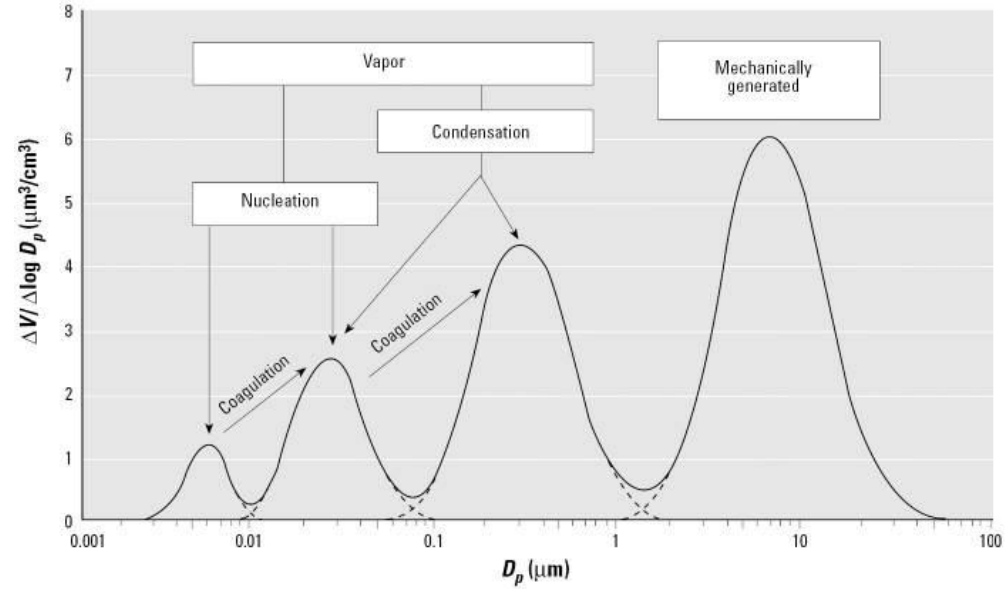
5 (reduced in 2021)

# Mechanisms

## Nanotoxicology: An Emerging Discipline Evolving from Studies of Ultrafine Particles

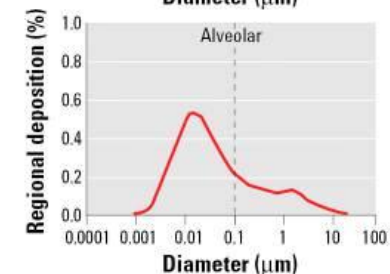
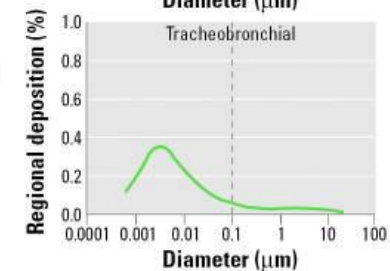
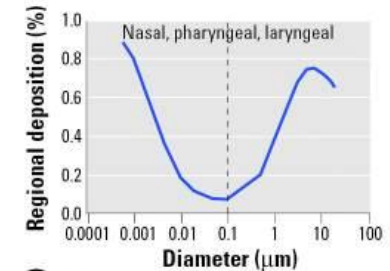
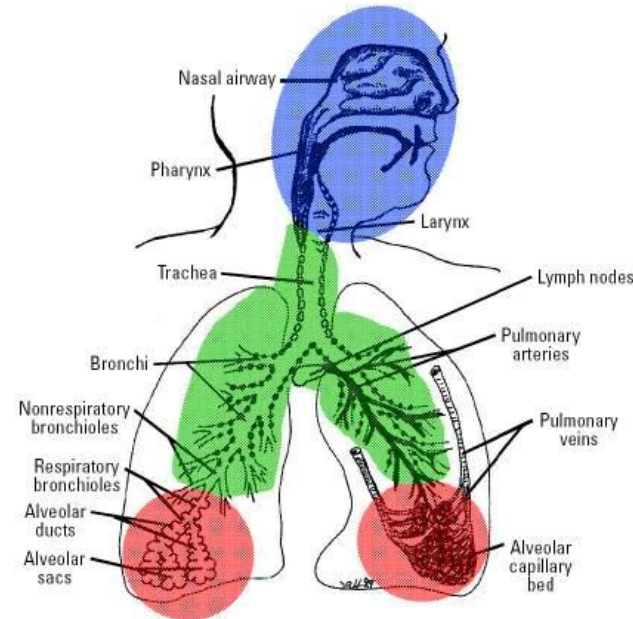
Günter Oberdörster,<sup>1</sup> Eva Oberdörster,<sup>2</sup> and Jan Oberdörster<sup>3</sup>

<sup>1</sup>Department of Environmental Medicine, University of Rochester, Rochester, New York, USA; <sup>2</sup>Department of Biology, Southern Methodist University, Dallas, Texas, USA; <sup>3</sup>Toxicology Department, Bayer CropScience, Research Triangle Park, North Carolina, USA



## Deposited particles

- mucocilliary clearance
- dissolution and blood stream
- translocation



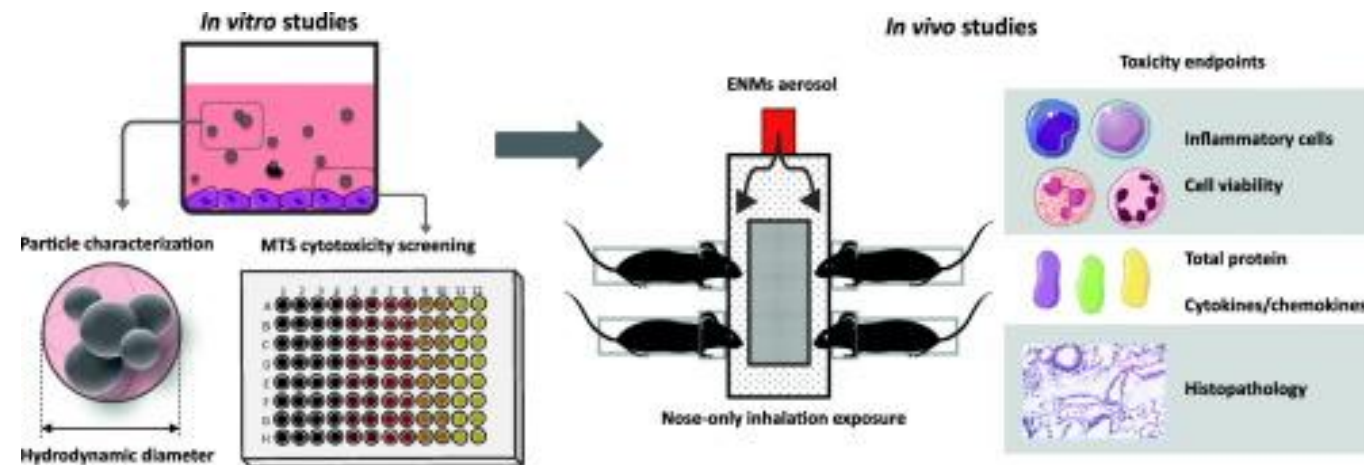
# Toxicity studies

## *in vitro*

- acellular / chemical assays
- cellular / biological assays

## *in vivo*

- human subjects
- other animal subjects



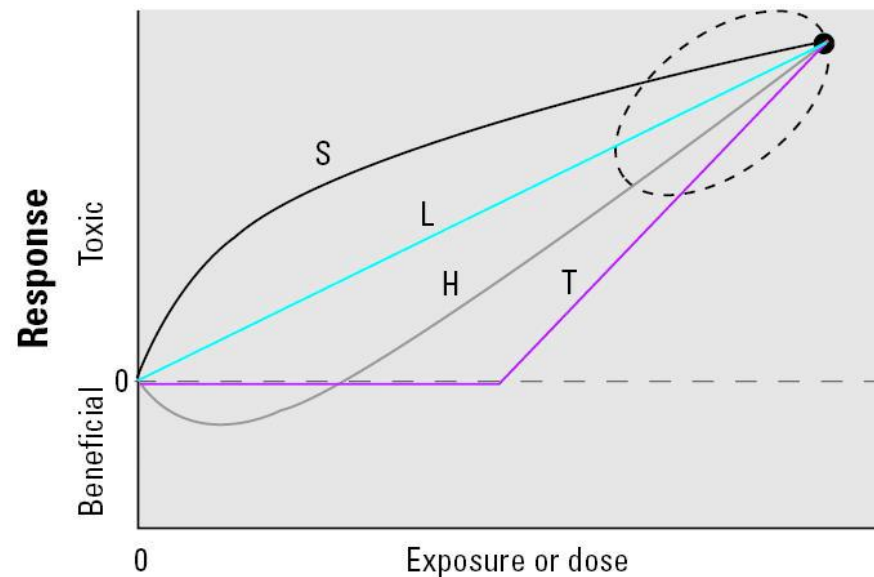
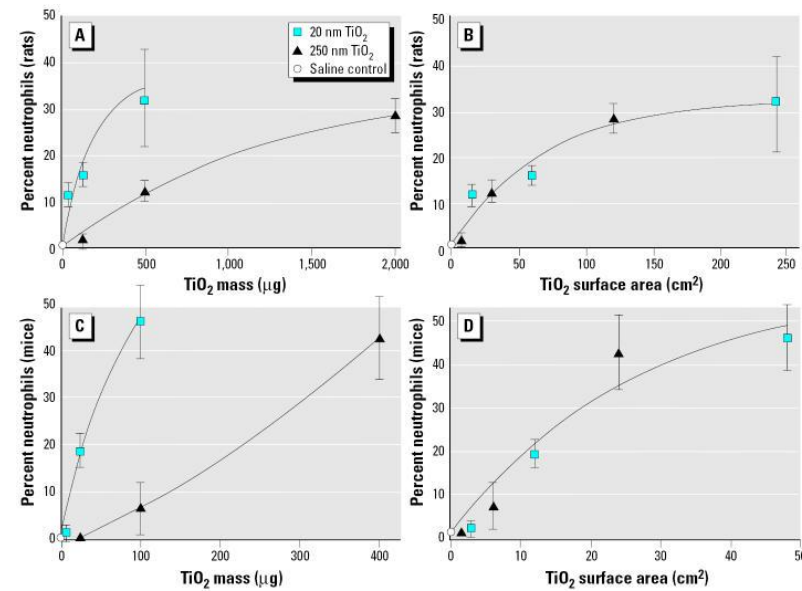
Areecheewakul et al., *Nanoimpact*, 2020

## Nanotoxicology: An Emerging Discipline Evolving from Studies of Ultrafine Particles

Günter Oberdörster,<sup>1</sup> Eva Oberdörster,<sup>2</sup> and Jan Oberdörster<sup>3</sup>

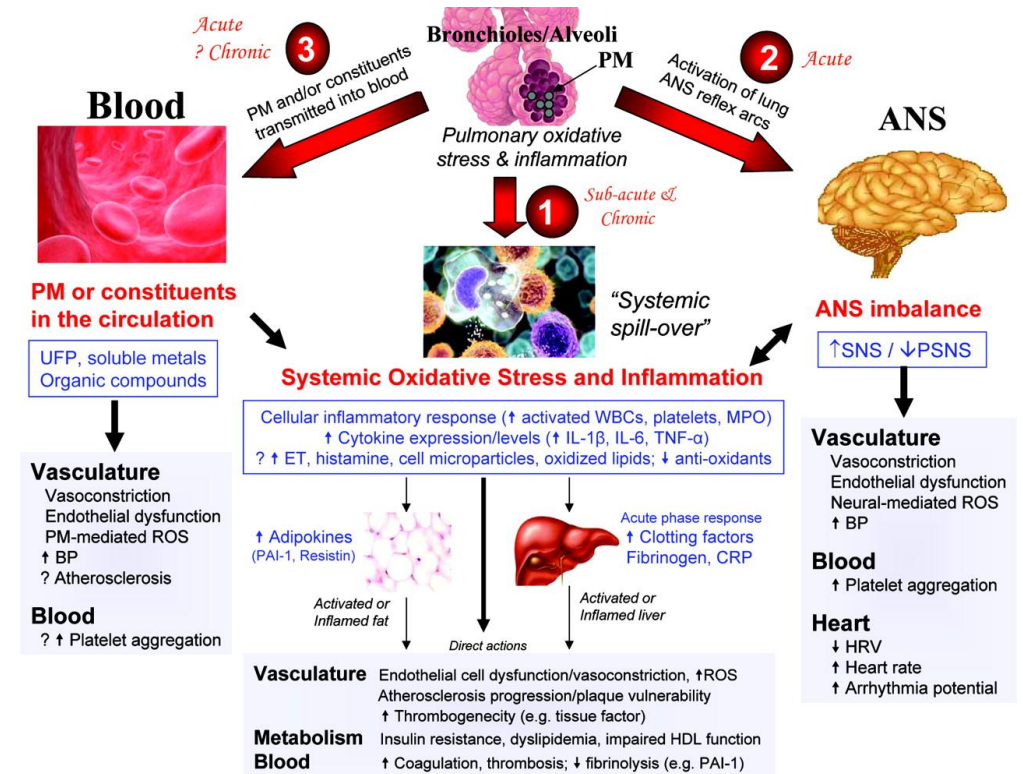
<sup>1</sup>Department of Environmental Medicine, University of Rochester, Rochester, New York, USA; <sup>2</sup>Department of Biology, Southern Methodist University, Dallas, Texas, USA; <sup>3</sup>Toxicology Department, Bayer CropScience, Research Triangle Park, North Carolina, USA

- High dose and exposure concentrations
- Short timescale of experiments
- Interpolation to low concentrations



# Some hypotheses

- mass concentrations
- ultrafine particles
- particle acidity
- transition metals
- oxidative stress



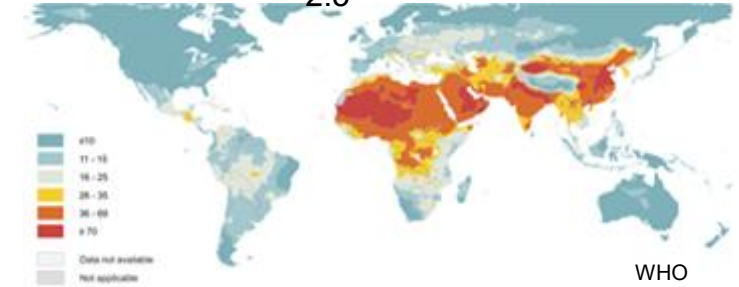
Brooks et al., *Circulation*, 2010

# Aerosol monitoring

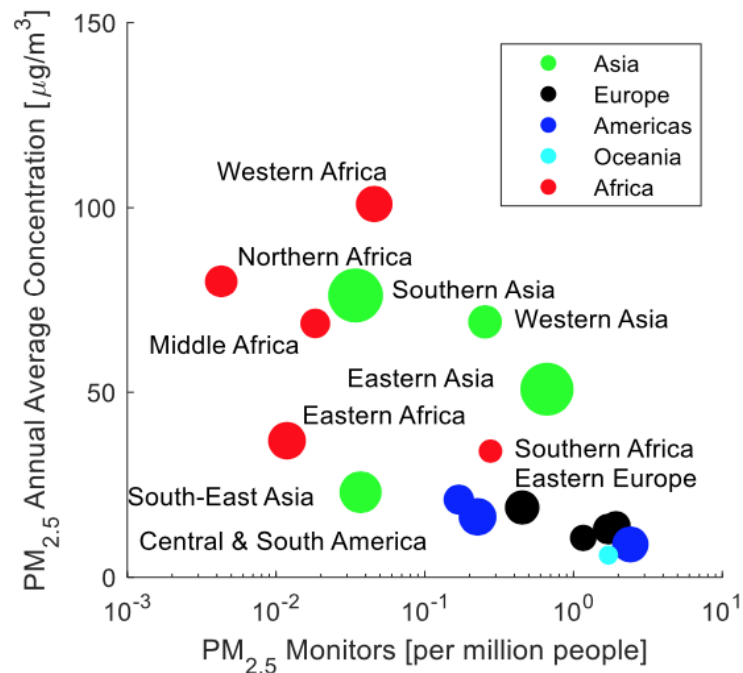
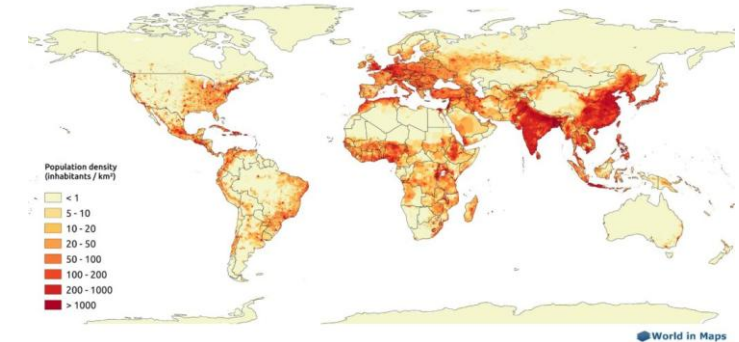
# Need for cost-effective monitoring of air pollution

(especially chemically resolved aerosol composition)

## Estimated PM<sub>2.5</sub> concentrations



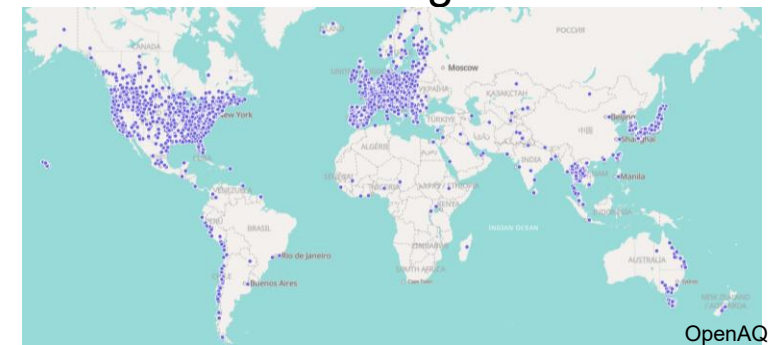
## Population density



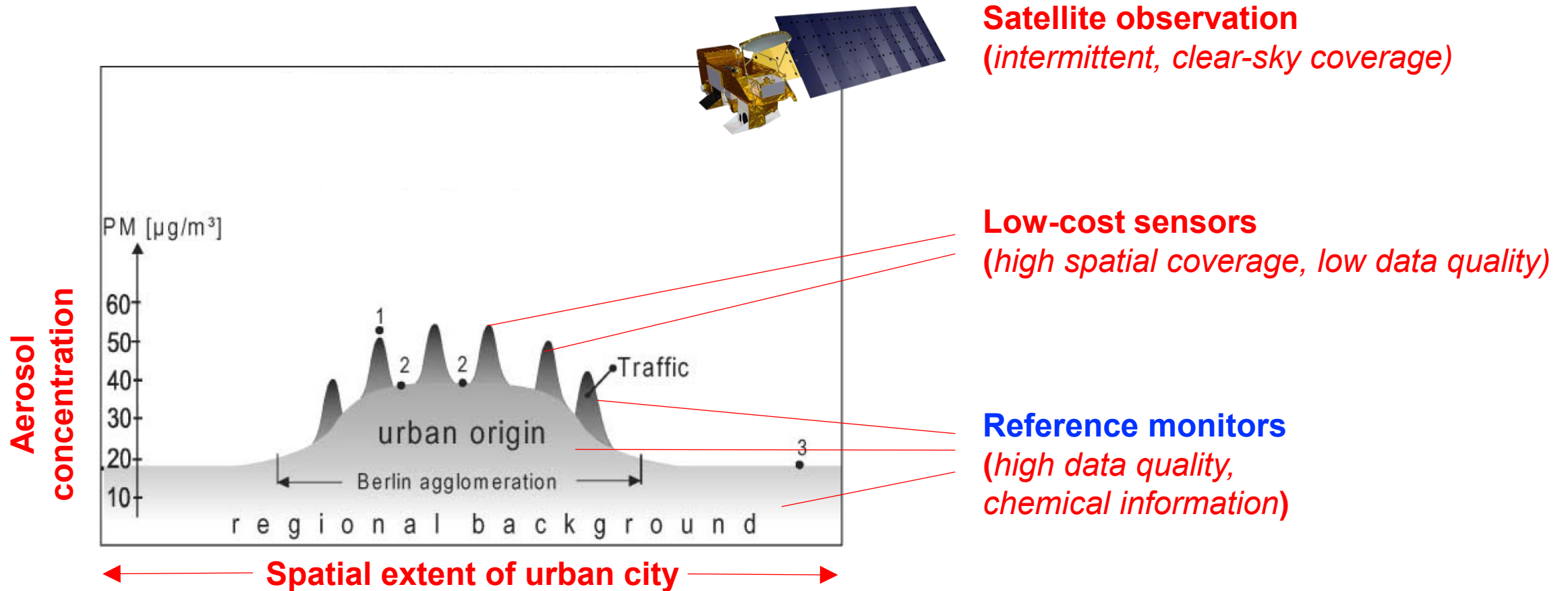
*Lack of monitors in high population areas*

Malings et al., 2020

## Available monitoring data



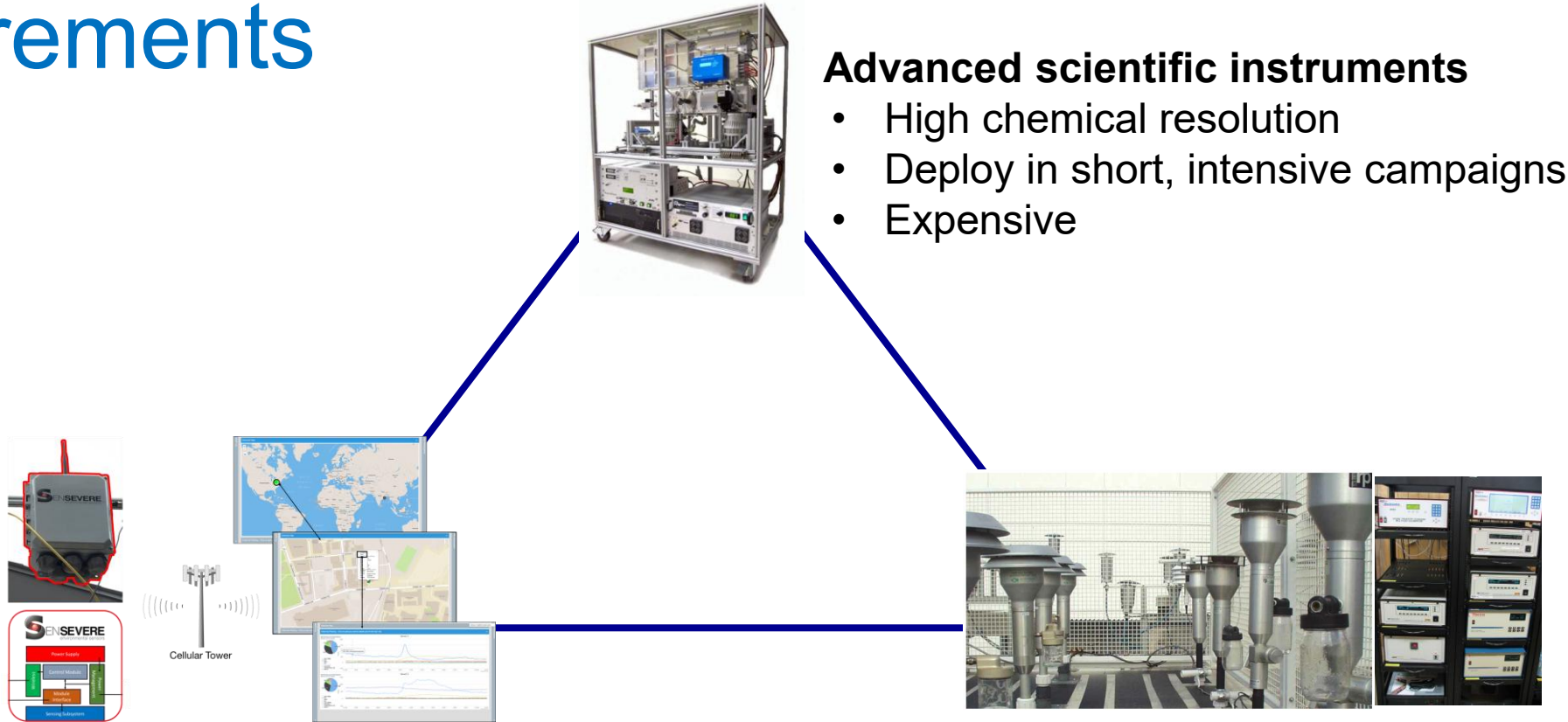
# Complementary monitoring strategies



# Chemical measurement technology tradeoffs

- offline / online
- time resolution
- chemical resolution (number of species)
- quantitative / qualitative
- physical / chemical separation vs algorithmic separation
- scalability – labor and cost

# Ground-based aerosol measurements



## Advanced scientific instruments

- High chemical resolution
- Deploy in short, intensive campaigns
- Expensive

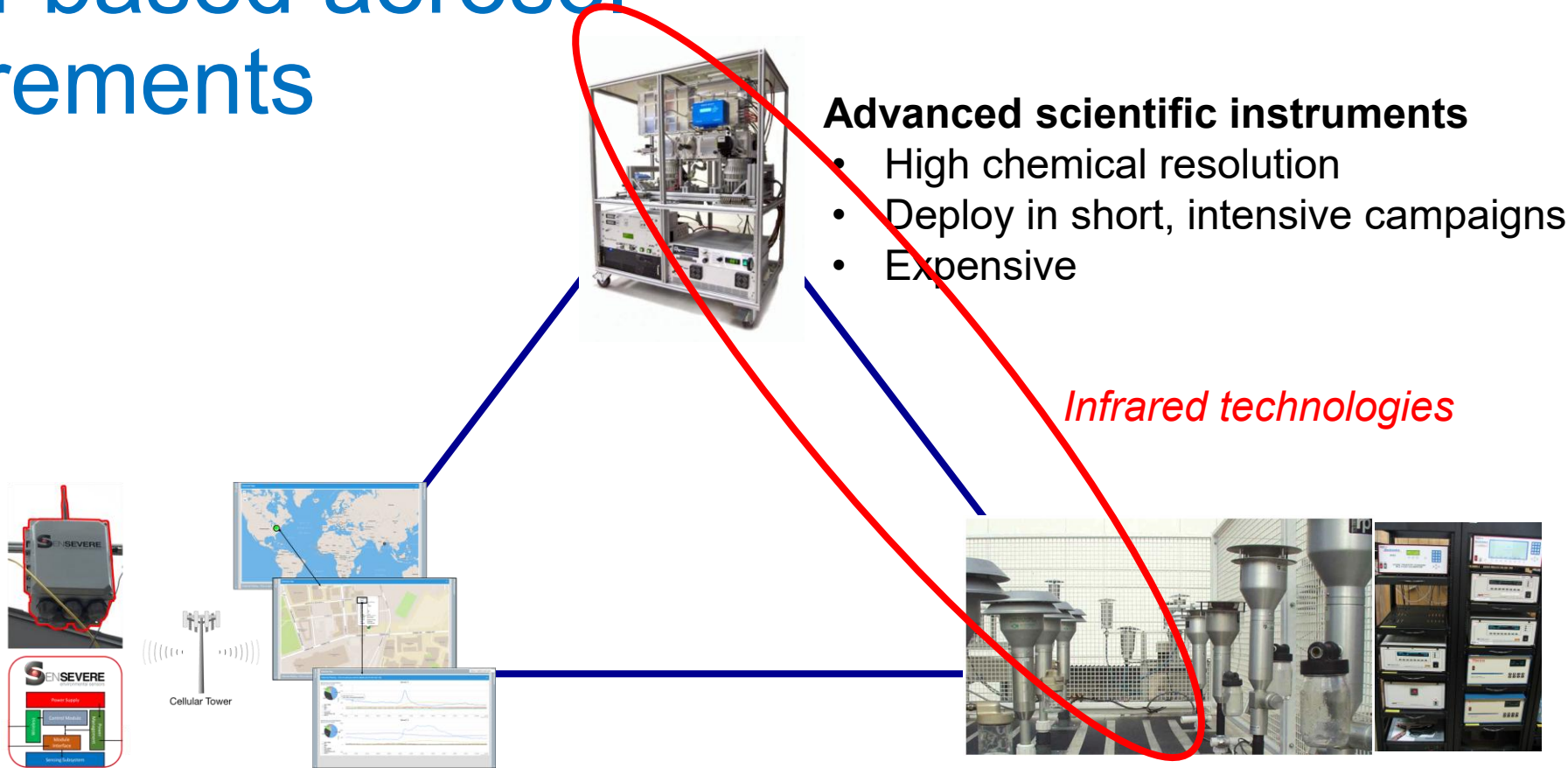
## Low-cost sensors

- High spatial (and time) resolution
- Personalized information (“citizen science”)
- No chemical information, low accuracy

## Regulatory monitors

- Reliable, standardized
- Accurate
- Cost-effective
- Chemical speciation

# Ground-based aerosol measurements



## Low-cost sensors

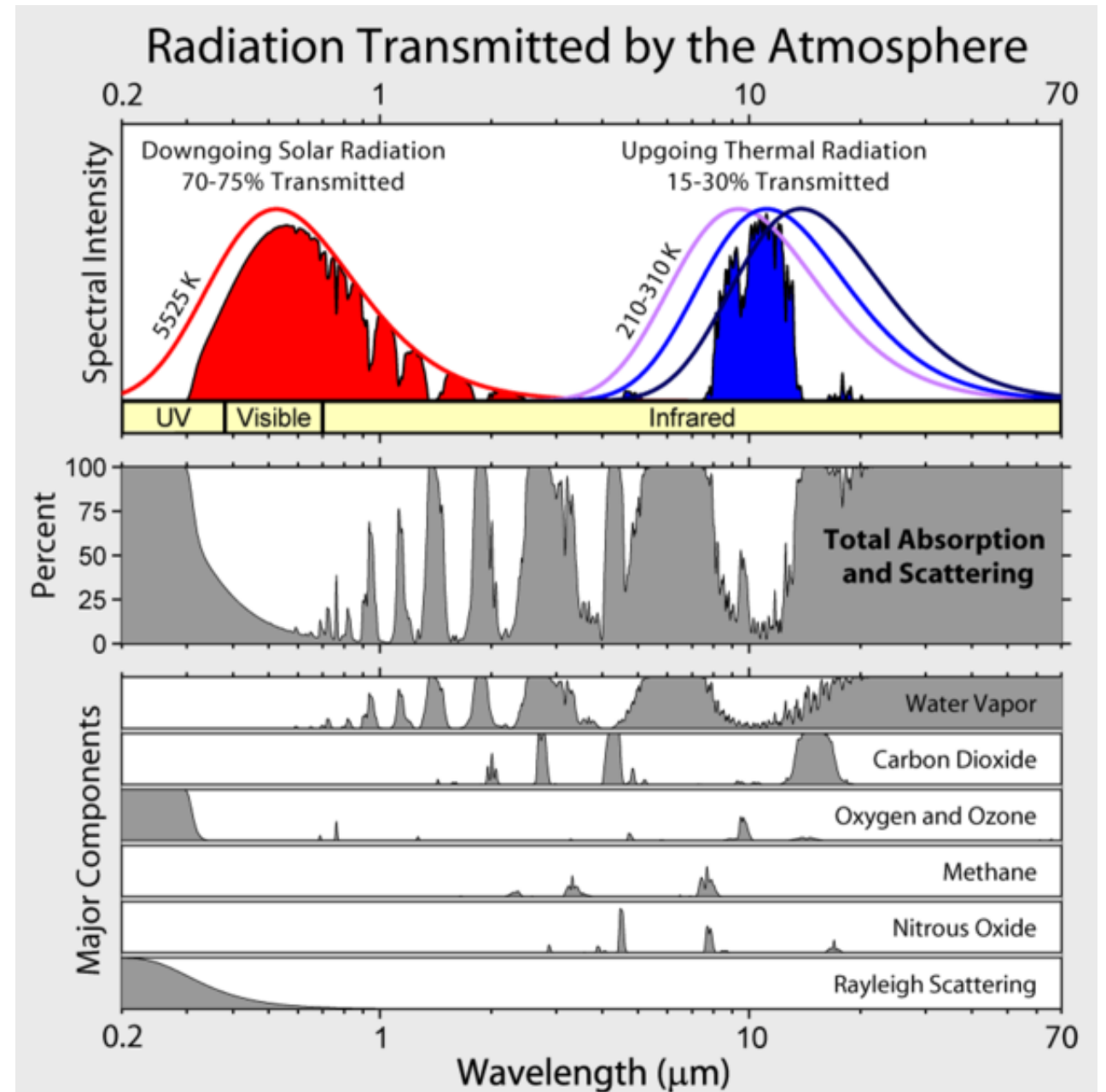
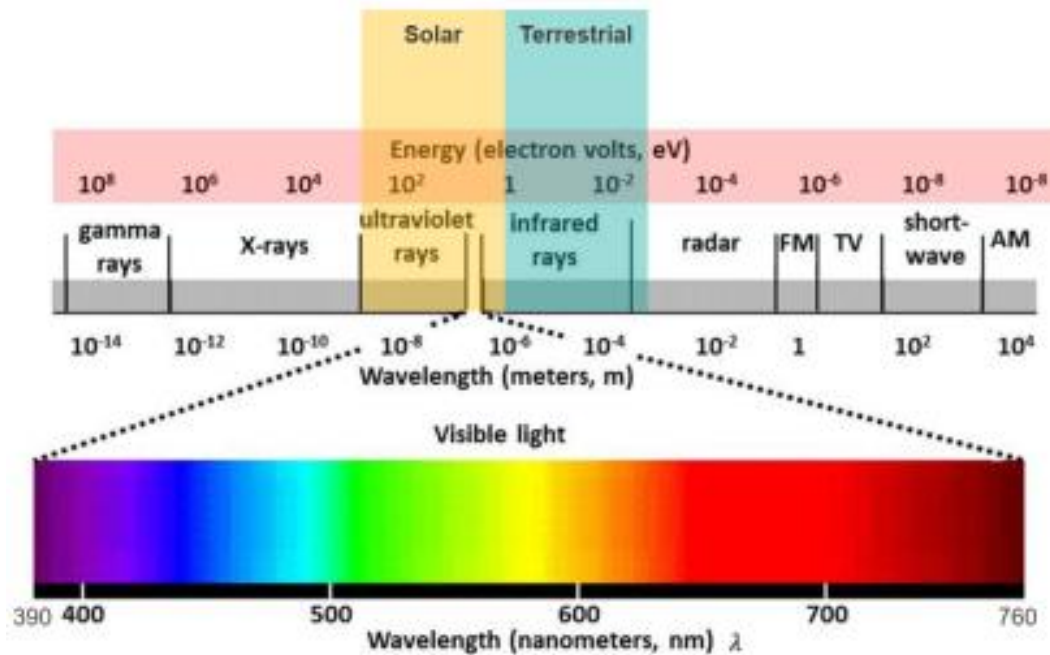
- High spatial (and time) resolution
- Personalized information (“citizen science”)
- No chemical information, low accuracy

## Regulatory monitors

- Reliable, standardized
- Accurate
- Cost-effective
- Chemical speciation

Measuring chemicals with  
infrared (thermal / mid-infrared)  
light-matter interactions

# Electromagnetic spectrum



# Absorption

An oscillating dipole can absorb energy from an oscillating electric field if the field also oscillates at the same frequency.

- ▶ a molecular dipole moment occurs because of unequal sharing of electrons
- ▶ electron densities of molecules are often approximated by point charges on atoms

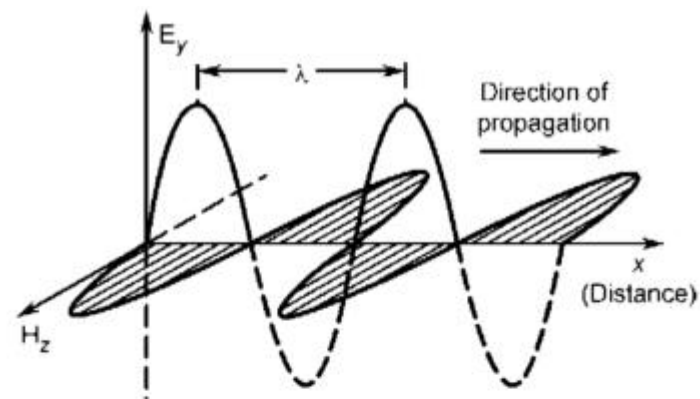
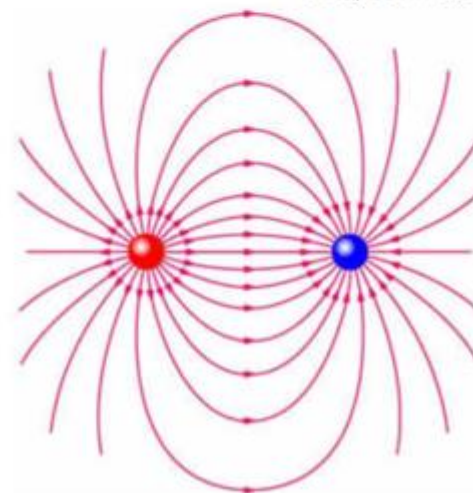
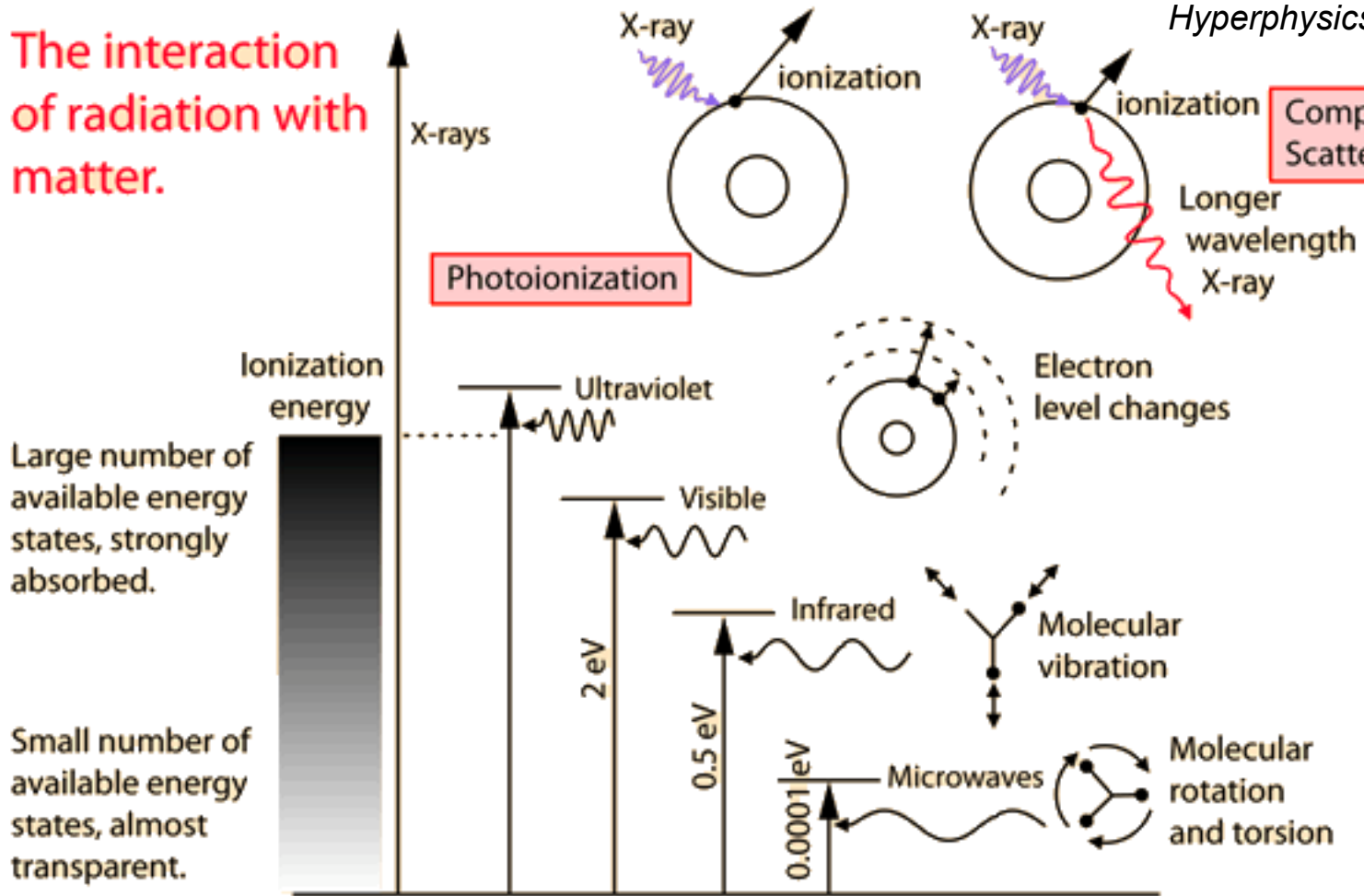


FIGURE 3.10 The instantaneous electric ( $E_y$ ) and magnetic ( $H_z$ ) field strength vectors of a plane-polarized light wave as a function of position along the axis of propagation ( $x$ ) (from Calvert and Pitts, 1966).

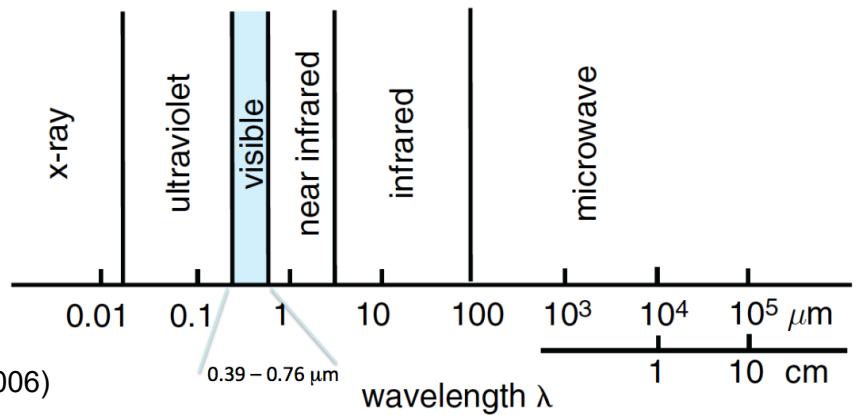
Finlayson-Pitts and Pitts, 1999



# The interaction of radiation with matter.



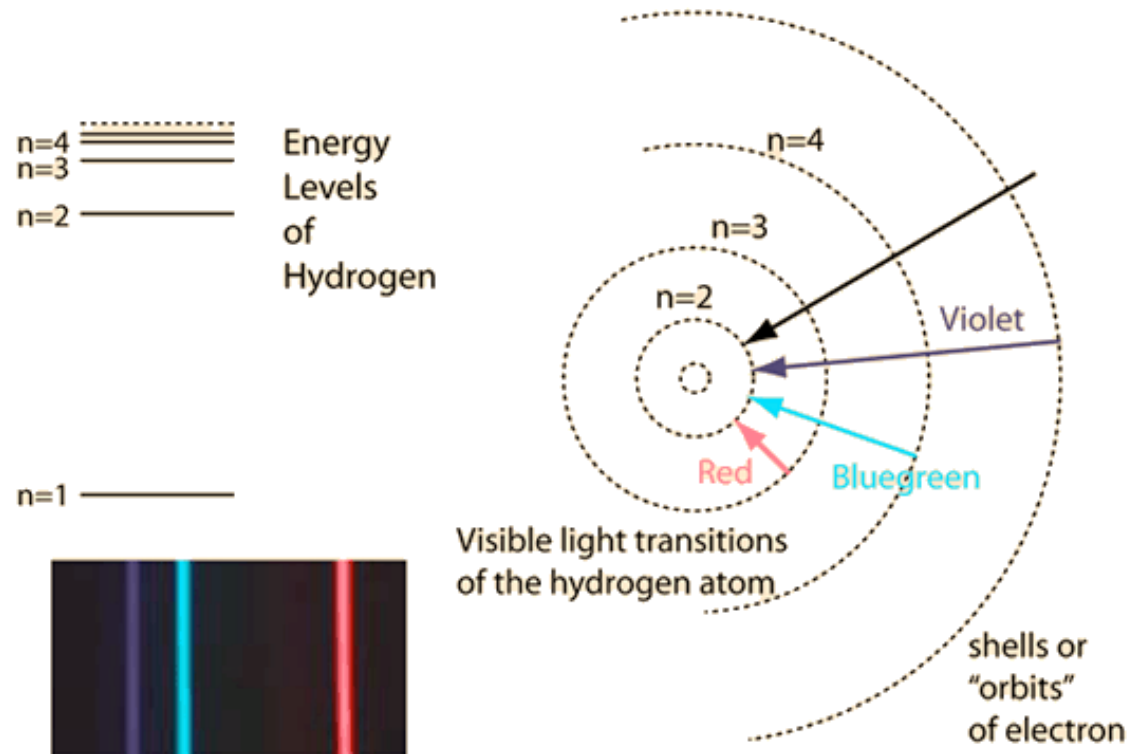
Wavelength (nm)	Description	Transition
~0.0003–0.03	γ-rays	nuclear
~0.03–10	X-rays	core electrons
~30–400	UV	valence electrons
~400–800	Visible	valence electrons
~1000–3 × 10 <sup>5</sup>	Infrared	molecular vibration
~3 × 10 <sup>7</sup> –3 × 10 <sup>11</sup>	Microwave	molecular rotation
~3 × 10 <sup>11</sup> –3 × 10 <sup>13</sup>	Radio	nuclear spin



Relationship between wavelength, energy, and frequency:

$$E = \frac{hc}{\lambda} = h\nu$$

# Conceptual model 1: Bohr's model of the atom



Hyperphysics, Georgia State Univ.

## Ultraviolet radiation

- electronic transitions (non-ionizing) induce excited states
- Ionizing at higher energies (*sunburn and skin cancer*)

## Visible radiation

- electronic transitions induce excited states

# Conceptual model 2: (an)harmonic oscillators

**Infrared radiation** induces changes in vibrational and rotational motion

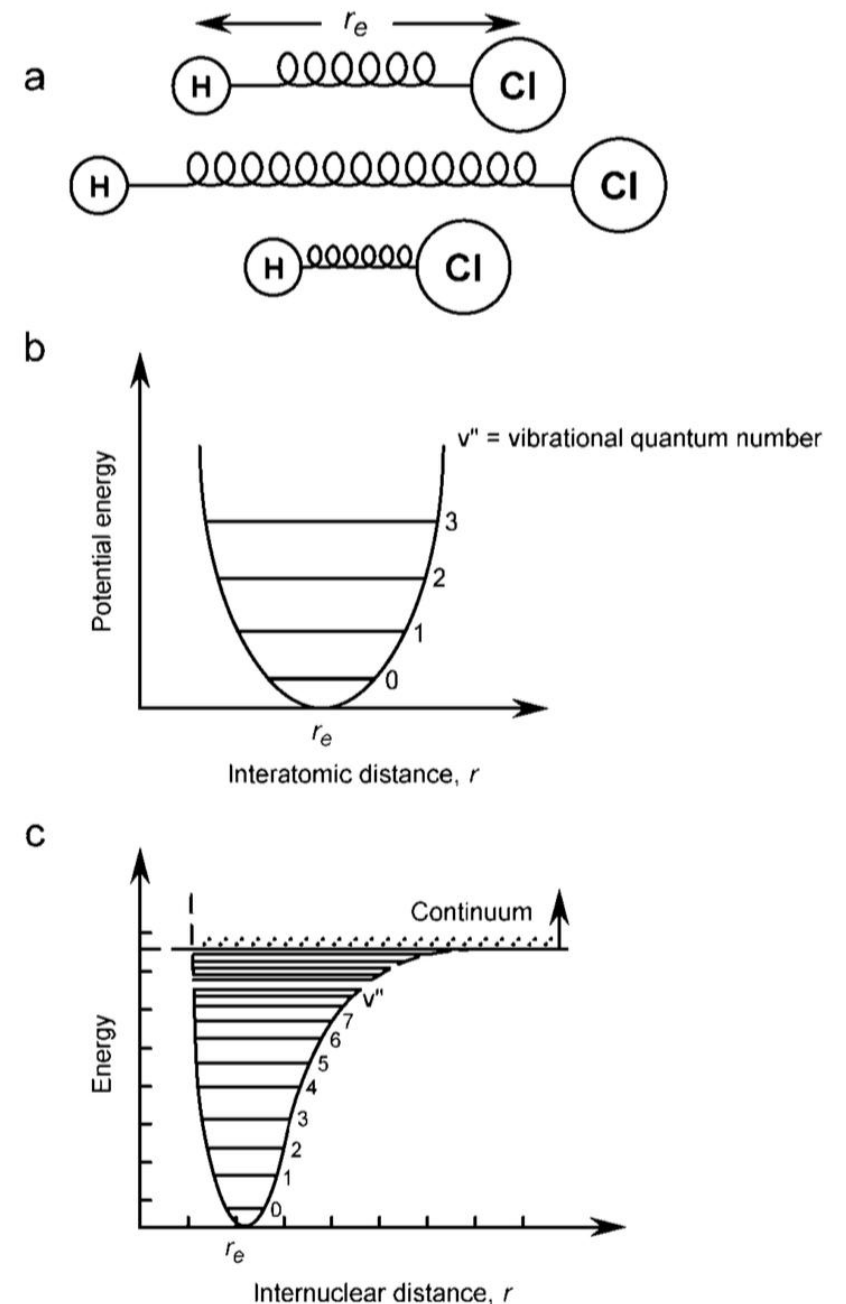
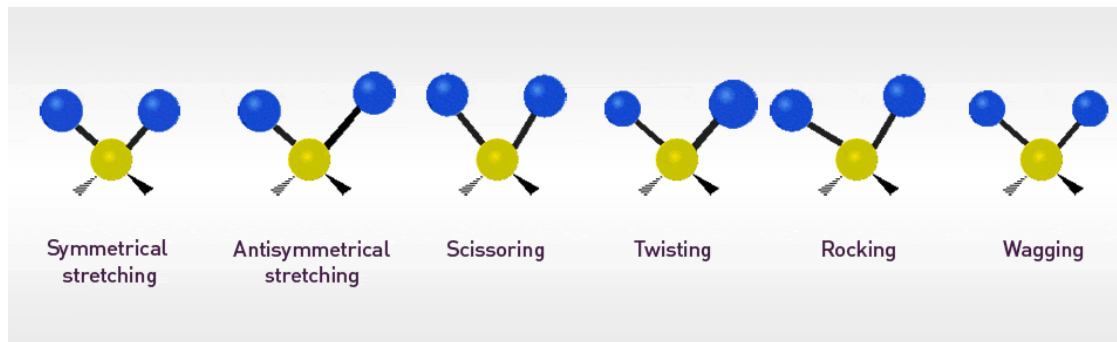


**FIGURE 3.2** (a) Vibration of diatomic molecule, HCl, (b) potential energy of an ideal harmonic oscillator, and (c) an anharmonic oscillator described by the Morse function.

# Most major constituents of atmospheric aerosols have absorption bands in the mid-infrared

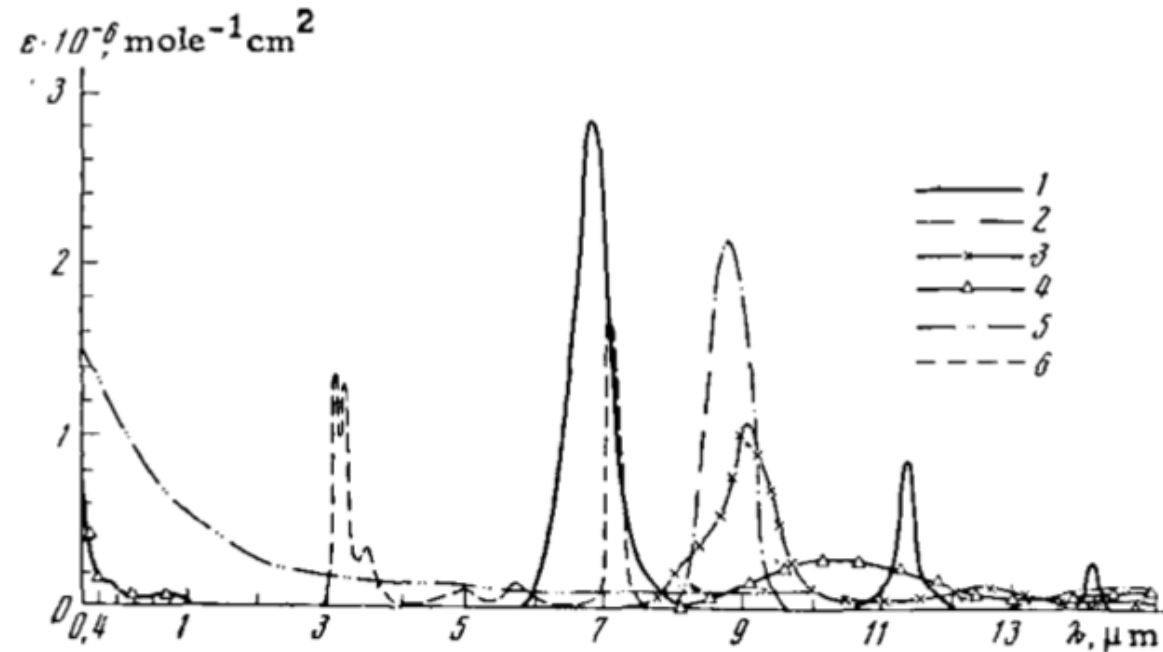
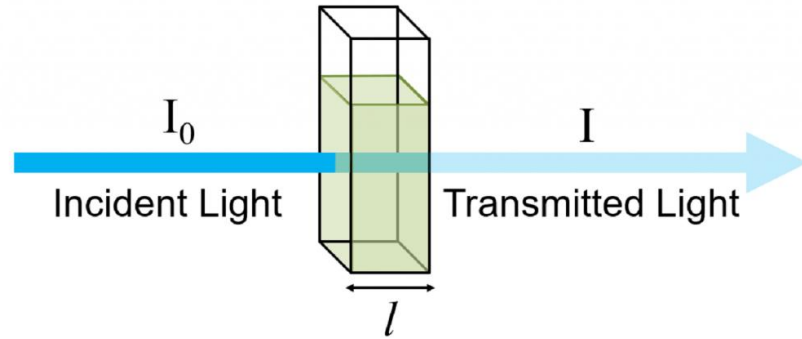


Fig. 5. Molar coefficients of absorption of the most important constituents of the atmospheric aerosol: 1) carbonate class; 2) sulfate class; 3) silicates; 4) amorphous hematite; 5) carbon black; 6) ammonium group.

# Detection and quantification via Bouguer-Lambert-Beer law



## Bouguer-Lambert-Beer law of absorption

$$dI(\tilde{\nu}) = -N \sigma(\tilde{\nu}) I ds$$

$$\int_{I_0}^I dI(\tilde{\nu}) = - \int_0^{\ell} N \sigma(\tilde{\nu}) I ds$$

$$T(\tilde{\nu}) = \frac{I(\tilde{\nu})}{I_0(\tilde{\nu})} = e^{-N \sigma(\tilde{\nu}) \ell}$$

$$A(\tilde{\nu}) = -\log T(\tilde{\nu}) = N \sigma(\tilde{\nu}) \ell$$

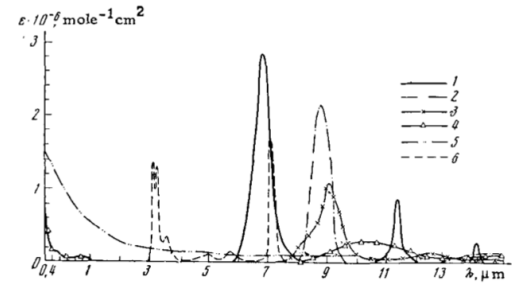
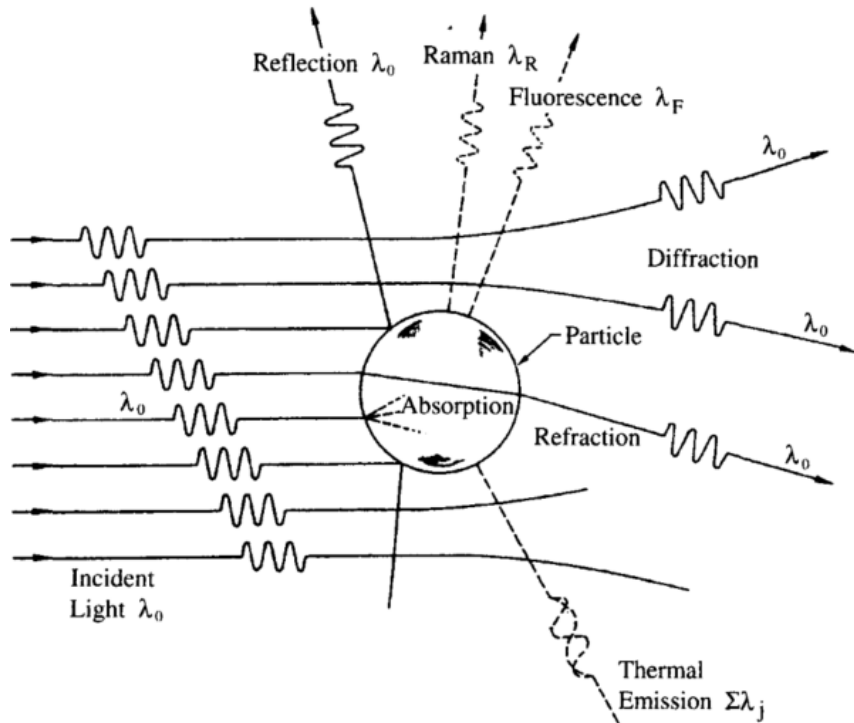


Fig. 5. Molar coefficients of absorption of the most important constituents of the atmospheric aerosol: 1) carbonate class; 2) sulfate class; 3) silicates; 4) amorphous hematite; 5) carbon black; 6) ammonium group.

Symbol	Description	Units
$\tilde{\nu}$	wavenumber	$\text{cm}^{-1}$
$I$	intensity (radiant flux)	$\text{W m}^{-2}$
$N$	number density	$\text{cm}^{-3}$
$\sigma$	absorption cross section	$\text{cm}^2$
$\ell$	path length	m
$T$	transmittance	
$A$	absorbance	

# Radiative transfer models

## Modified BLB equations



Particles scatter radiation

$$\sigma \rightarrow \sigma_{\text{ext}} = \sigma_{\text{abs}} + \sigma_{\text{sca}}$$

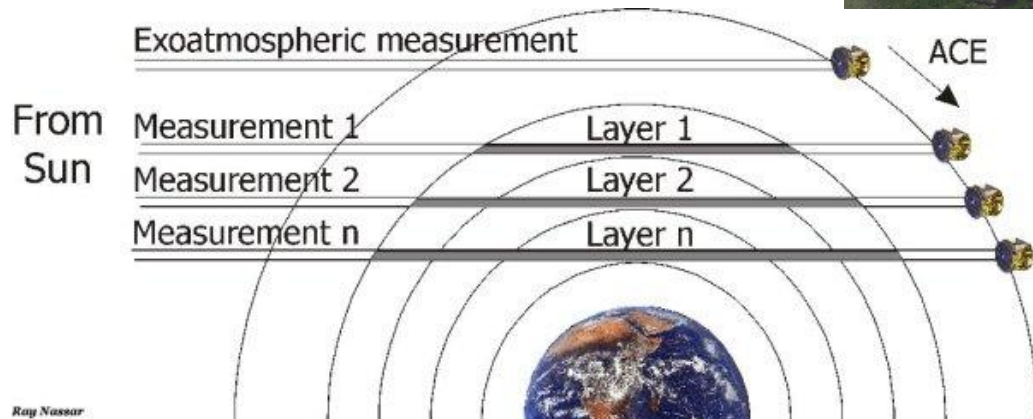
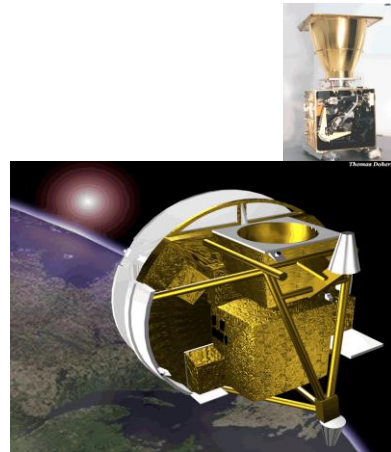
Atmosphere comprises multiple phases

$$A = \ell \left( \sum_{i \in \text{gases}} N_i \sigma_{\text{ext},i} + \sum_{i \in \text{particles}} N_i \sigma_{\text{ext},i} + \sum_{i \in \text{hydrometeors}} N_i \sigma_{\text{ext},i} \right)$$

# Applications to environmental monitoring / Earth Observation

# ACE-FTS aboard the SCISAT-1

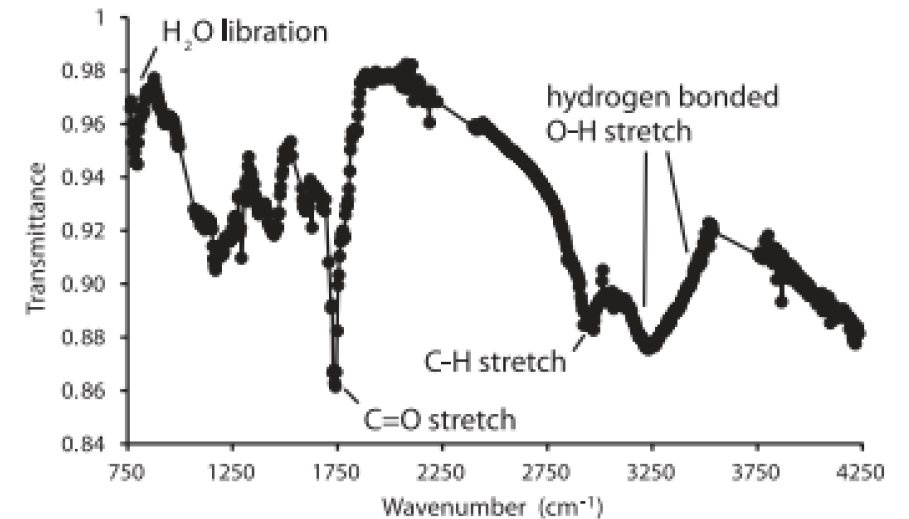
Atmospheric Chemistry Experiment – Fourier Transform Spectrometer



## WILDFIRES

### Wildfire smoke destroys stratospheric ozone

Peter Bernath<sup>1,2,3\*</sup>, Chris Boone<sup>2</sup>, Jeff Crouse<sup>2</sup>



Wavenumber  $\tilde{\nu} = \frac{1}{\lambda}$

<https://uwaterloo.ca/atmospheric-chemistry-experiment/mission/solar-occultation-orbit>

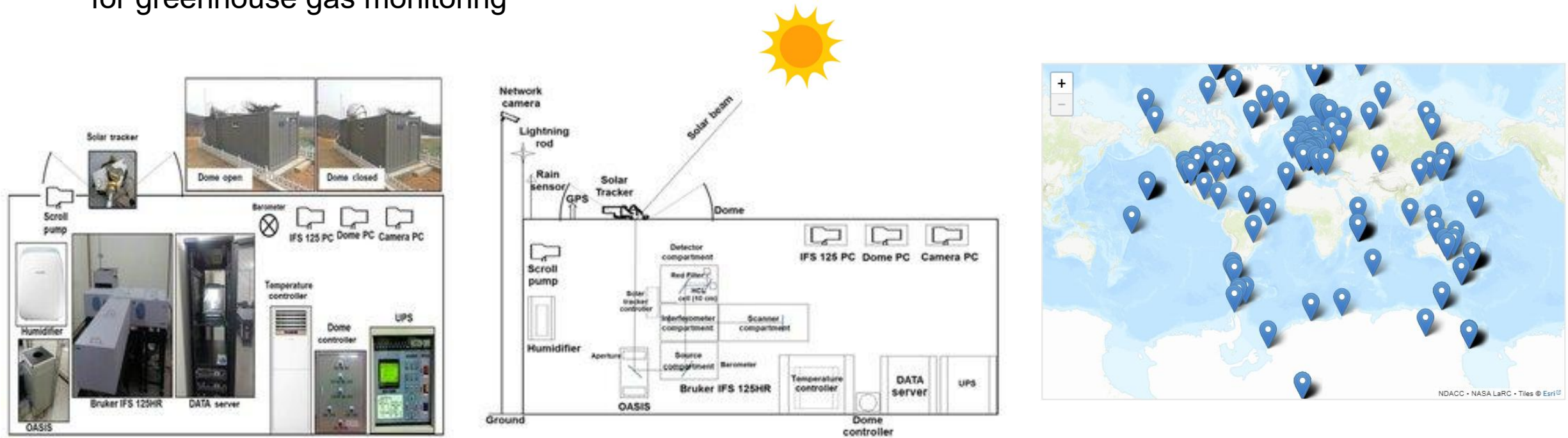
<https://uwaterloo.ca/atmospheric-chemistry-experiment/instruments/ace-fts>

<https://www.nasa.gov/image-article/scientific-satellite-atmospheric-chemistry-experiment-1-scisat-1/>

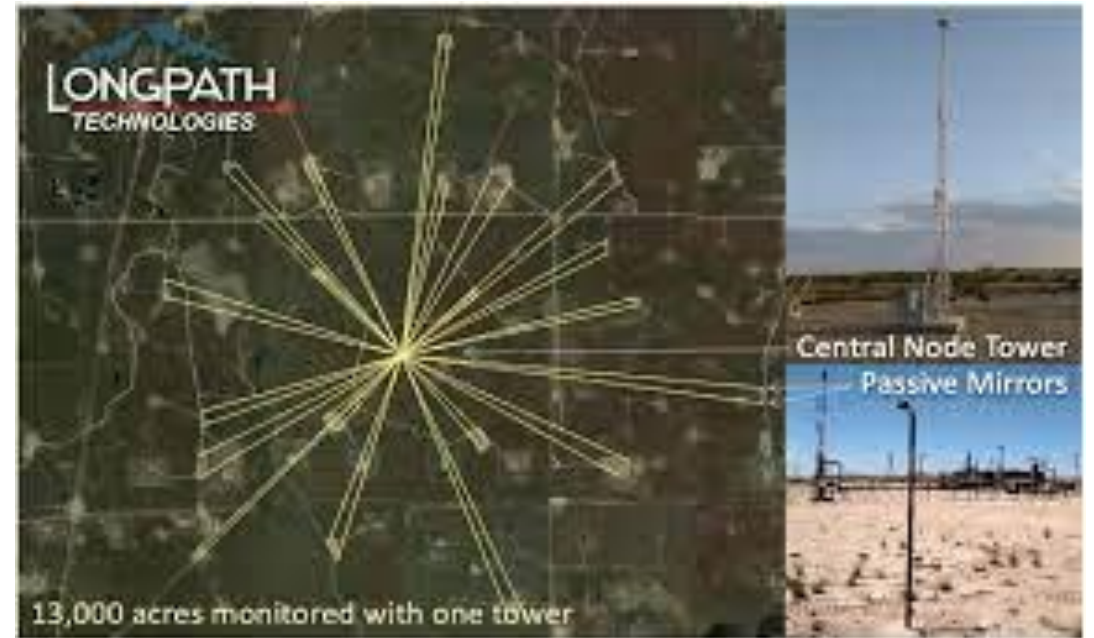
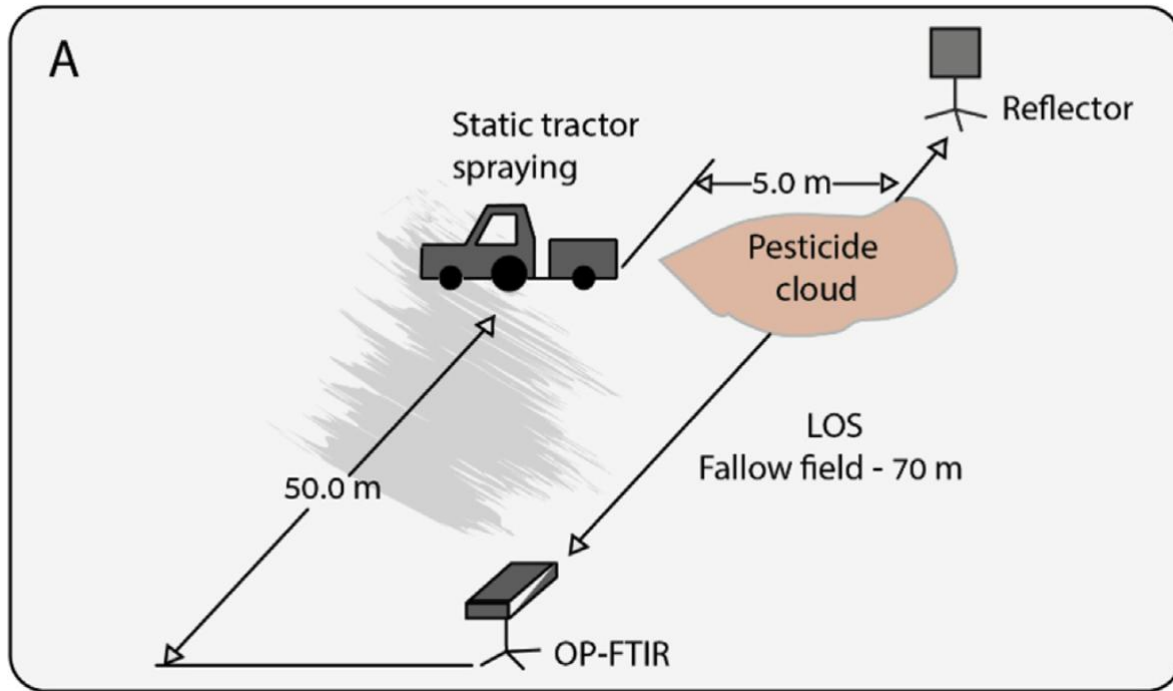
# Solar-viewing FTS in the NDACC

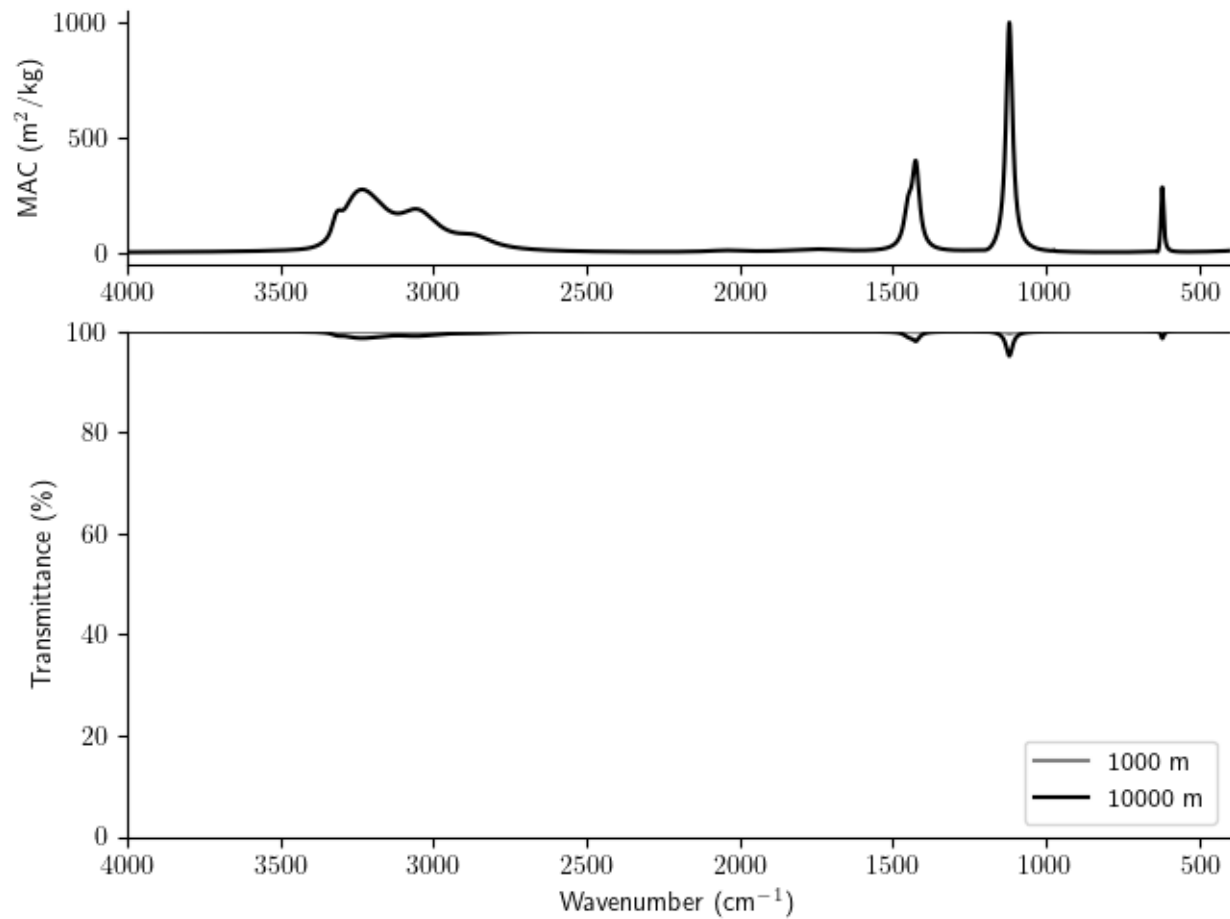
Network for the Detection of Atmospheric Composition Change

for greenhouse gas monitoring



# Open-path infrared (“standoff detection”)

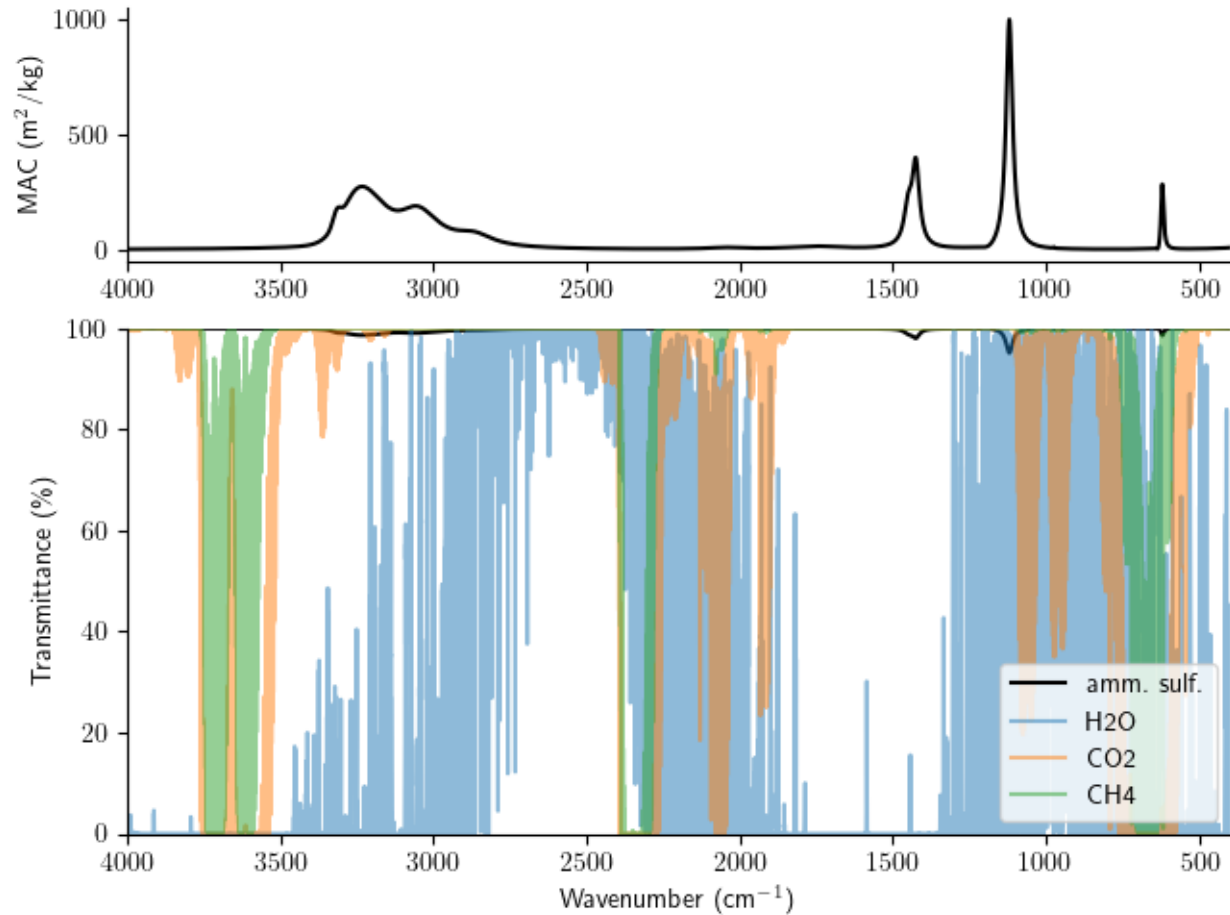




virtual experiment

➤ ammonium sulfate  $5 \mu\text{g}/\text{m}^3$

➤ path lengths 1 and 10 km



## virtual experiment

- ammonium sulfate 5  $\mu\text{g}/\text{m}^3$
- path length 10 km  
(*super-optimistic scenario*)
- H<sub>2</sub>O: 50%RH at 25 deg.C  
(11  $\text{g}/\text{m}^3$ )
- CO<sub>2</sub>: 420 ppm  
(0.8  $\text{g}/\text{m}^3$ )
- CH<sub>4</sub>: 1911 ppb  
(1  $\text{mg}/\text{m}^3$ )

# Advances in open path technologies

- High intensity source
- High spectral resolution (remove gas phase)
- Stable baseline
- Select applications

Proceedings  
of the  
Combustion  
Institute

Mid-infrared dual frequency comb spectroscopy for  
combustion analysis from 2.8 to 5  $\mu\text{m}$

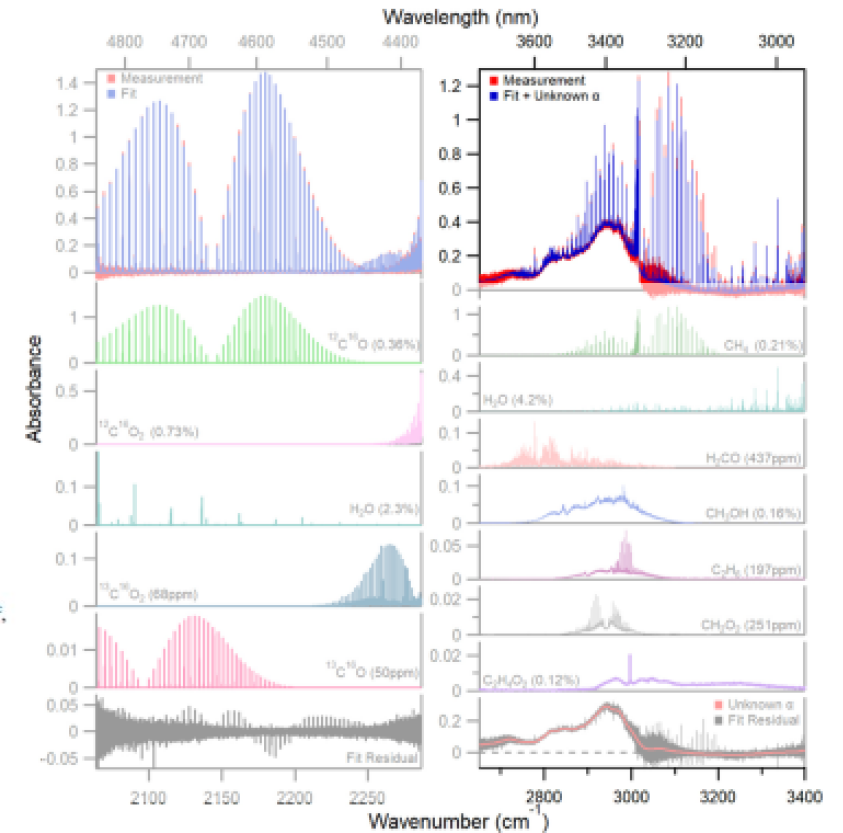
Amanda S. Makowiecki<sup>a</sup>, Daniel I. Herman<sup>b</sup>, Nazanin Hoghooghi<sup>a</sup>,  
Elizabeth F. Strong<sup>a</sup>, Ryan K. Cole<sup>a</sup>, Gabe Ycas<sup>c</sup>, Fabrizio R. Giorgetta<sup>c</sup>,  
Caelan B. Lapointe<sup>a</sup>, Jeffrey F. Glusman<sup>a</sup>, John W. Daily<sup>a</sup>,  
Peter E. Hamlington<sup>a</sup>, Nathan R. Newbury<sup>c</sup>, Ian R. Coddington<sup>c</sup>,  
Gregory B. Rieker<sup>a,\*</sup>

<sup>a</sup> Department of Mechanical Engineering, University of Colorado Boulder, Boulder, CO 80309, USA

<sup>b</sup> Department of Physics, University of Colorado Boulder, Boulder, CO 80309, USA

<sup>c</sup> National Institute of Standards and Technology, Boulder, CO 80305, USA

Received 7 November 2019; accepted 7 June 2020  
Available online 29 September 2020



# Standoff Aerosol Sensing with Mid-infrared Dual Frequency Comb Spectroscopy

Garrett C. Mathews<sup>\*1</sup>, Alyssa Lalko<sup>1</sup>, Anna Ziola<sup>1</sup>, Amanda Makowiecki<sup>2</sup>, Kevin Williamson<sup>2</sup>, Douglas Day<sup>1</sup>, Masayuki Takeuchi<sup>1</sup>, Scott Egbert<sup>1</sup>, Graeme Gillespie<sup>1</sup>, Anthony Harness<sup>2</sup>, Robert Wright<sup>2</sup>, Anne Handschy<sup>1</sup>, Nazanin Hoghooghi<sup>1,3</sup>, Peter Chang<sup>1</sup>, Satoshi Takahama<sup>1,4</sup>, Daven Henze<sup>1</sup>, Jose L. Jimenez<sup>1</sup>, Scott A. Diddams<sup>1,4</sup>, and Gregroy B. Rieker<sup>1,2</sup>

<sup>1</sup>University of Colorado Boulder, Boulder, CO 80309, USA

<sup>2</sup>LongPath Technologies, Boulder, CO 80301, USA

<sup>3</sup>National Institute of Standards and Technology, Boulder CO 80305, USA

<sup>4</sup>Ecole Polytechnique Fédérale de Lausanne, Lausanne, Switzerland

\*Email: garrett.mathews@colorado.edu

2025 Conference on Lasers and Electro-Optics (CLEO)

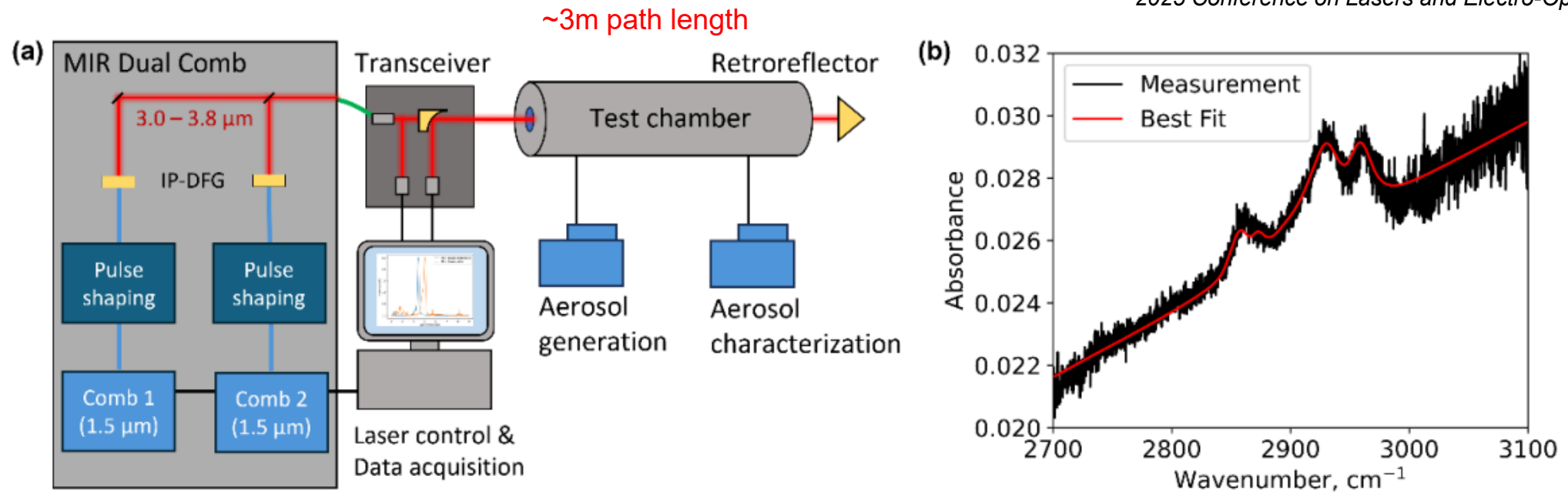
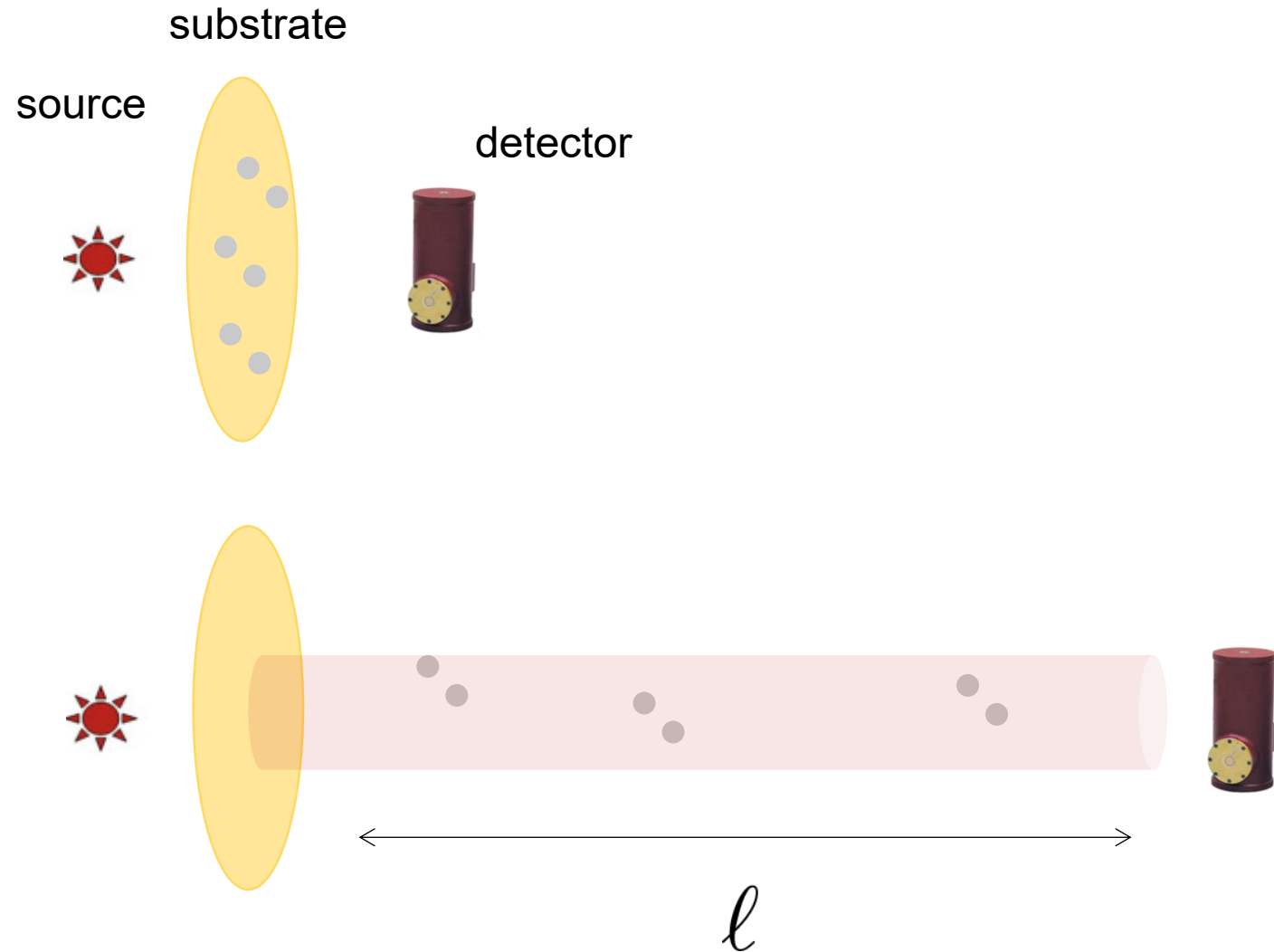


Figure 1: Experimental setup used to perform DCS measurements of aerosol absorption spectra (a). Measured and best-fit spectrum of aerosolized dioctyl sebacate (DOS) (b).

# Mid-infrared in aerosol chemical monitoring

# Particle collection for infrared sensing



areal number density

$$A = N^{(\text{area})} \sigma_{\text{ext}}$$

$$N^{(\text{area})} = N \ell$$

$$\ell = v_f t$$

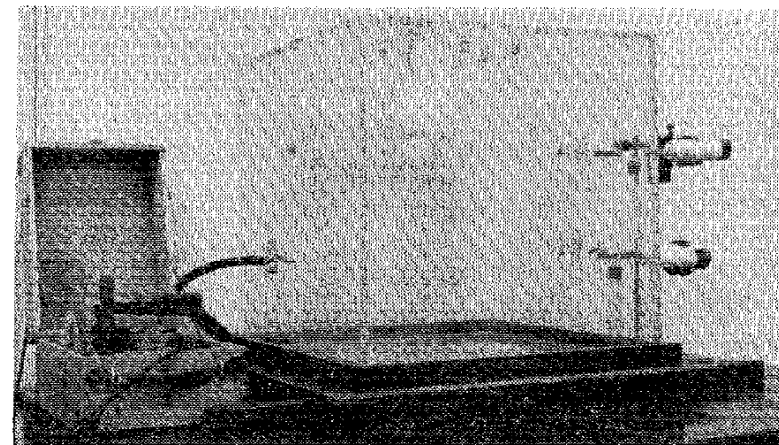
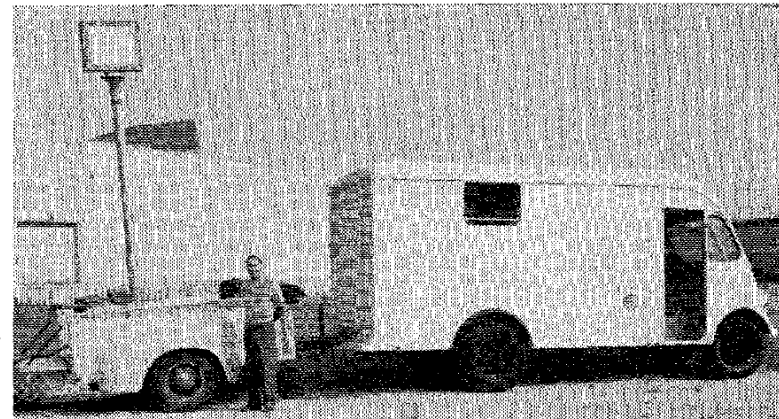
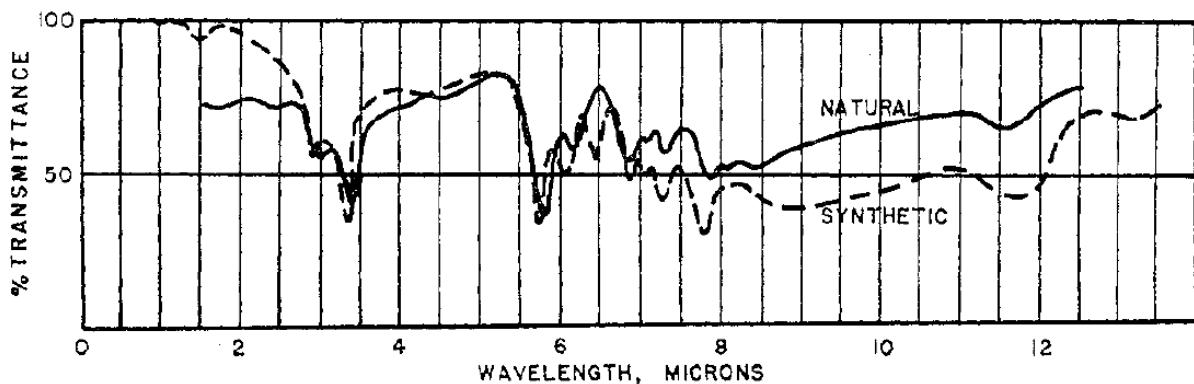
substrate face velocity

# Composition of Organic Portion of Atmospheric Aerosols in the Los Angeles Area

PAUL P. MADER, ROBERT D. MACPHEE,  
ROBERT T. LOFBERG, AND GORDON P. LARSON  
*Los Angeles County Air Pollution Control District, Los Angeles, Calif.*

June 1952

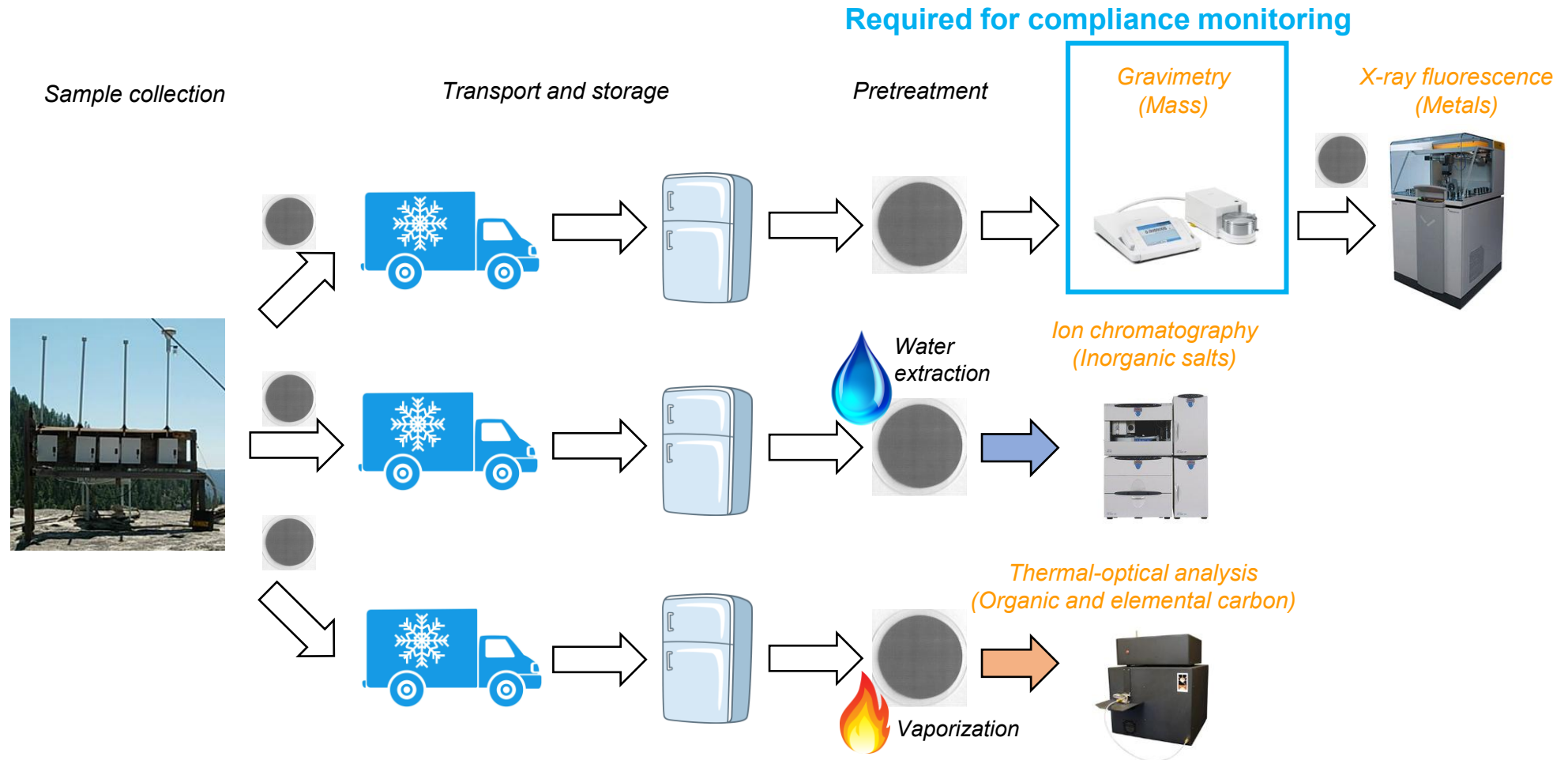
INDUSTRIAL AND ENGINEERING CHEMISTRY



...~45 years later →

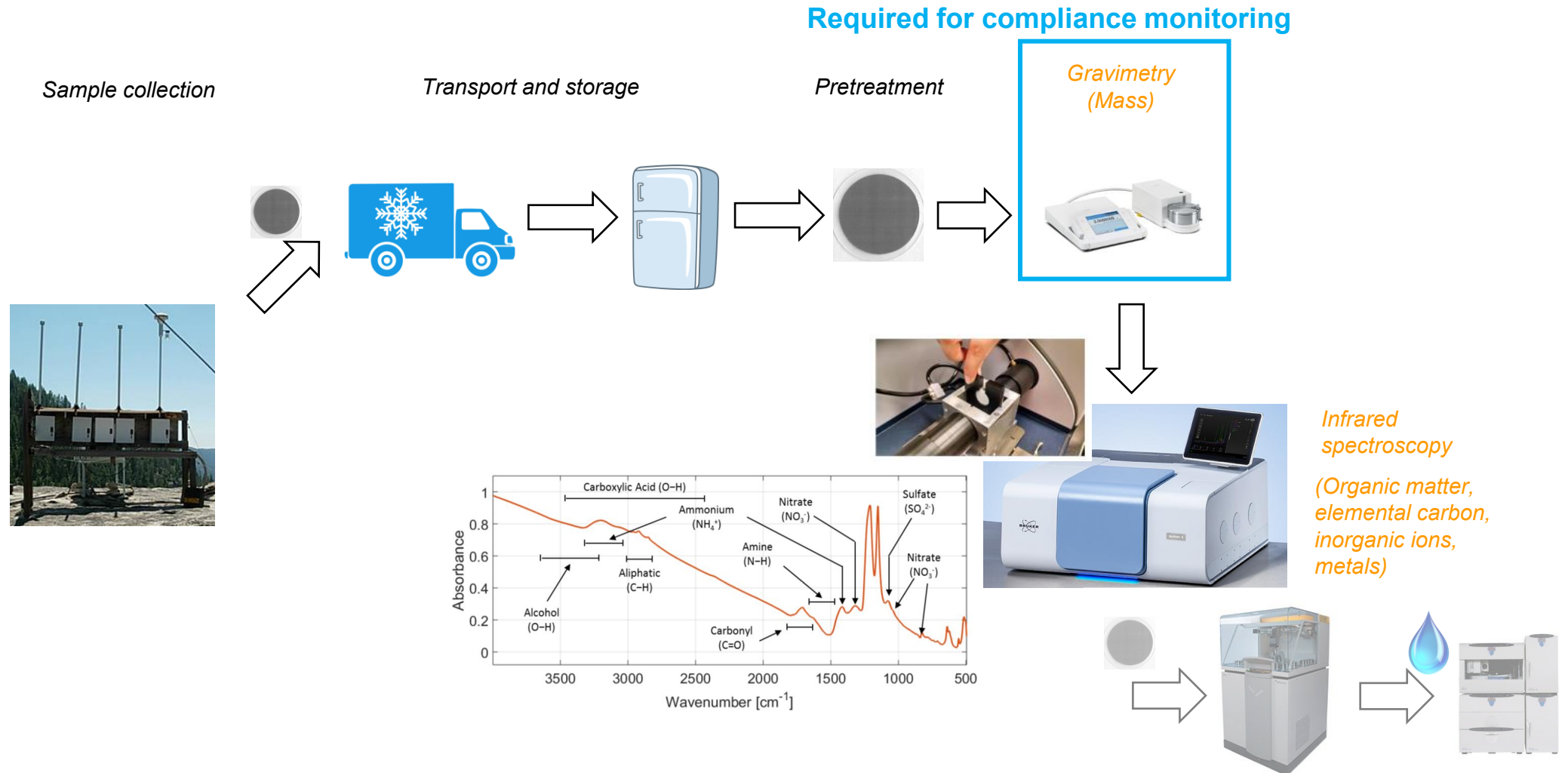
# Conventional chemical speciation methods

Laborious and costly



# Mid-infrared spectrometry

## Single analytical technique for chemical speciation



# Challenges for quantitative analysis of atmospheric aerosols with infrared

## Environmental infrared spectra is especially complex

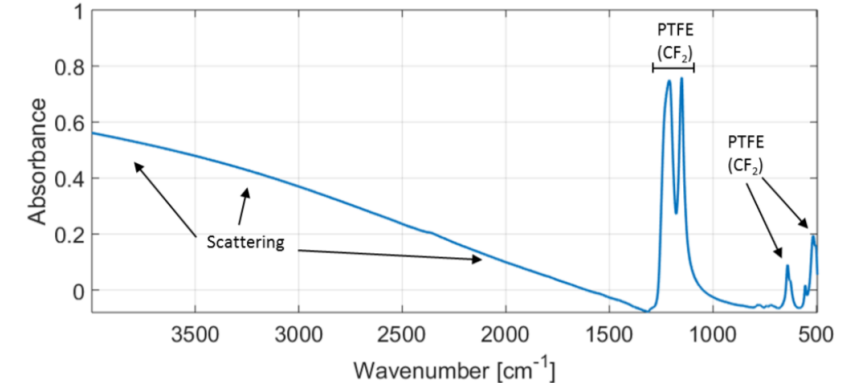
- heterogeneous media leading to scattering and other phenomena
- mixtures leading to overlapped peaks
- interference from substrate

## Algorithmic approach

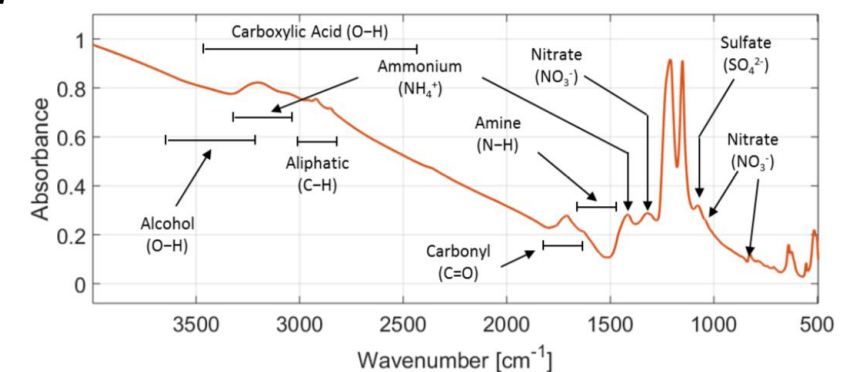
for quantitative analysis of atmospheric aerosols:

- ensure reliability across diverse samples in measurement network
- expert systems (first wave of AI)
- data-drive modeling (machine learning)

*blank Teflon filter*



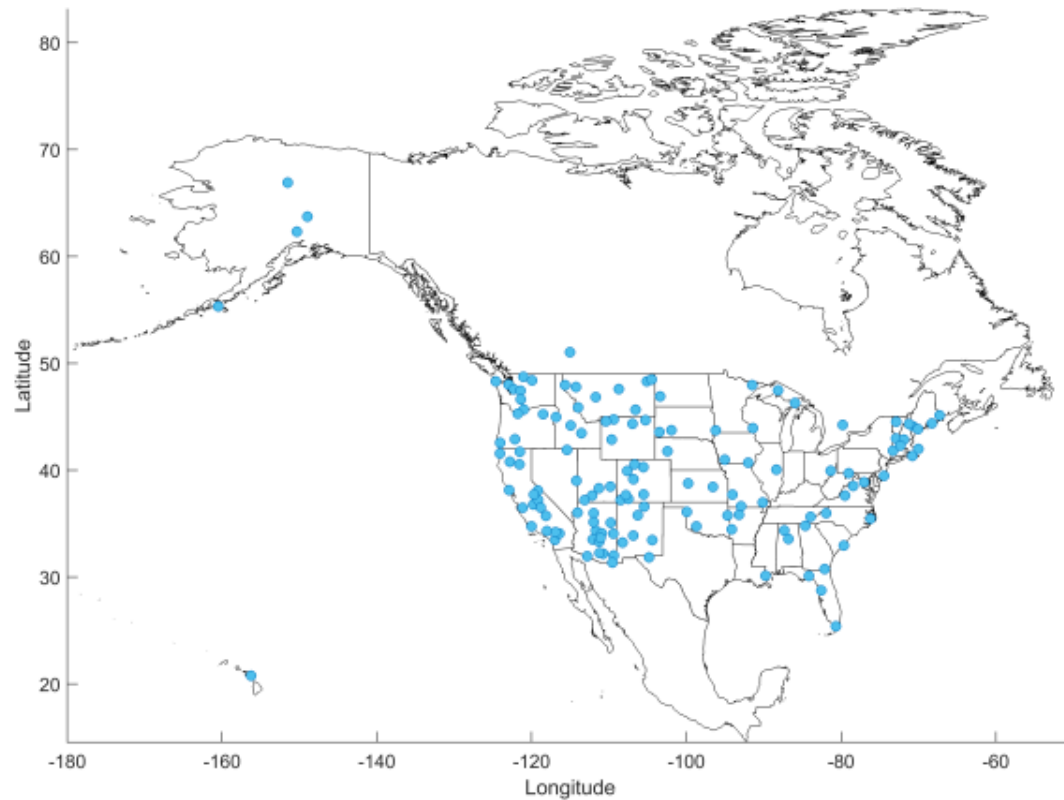
*particle-loaded filter*



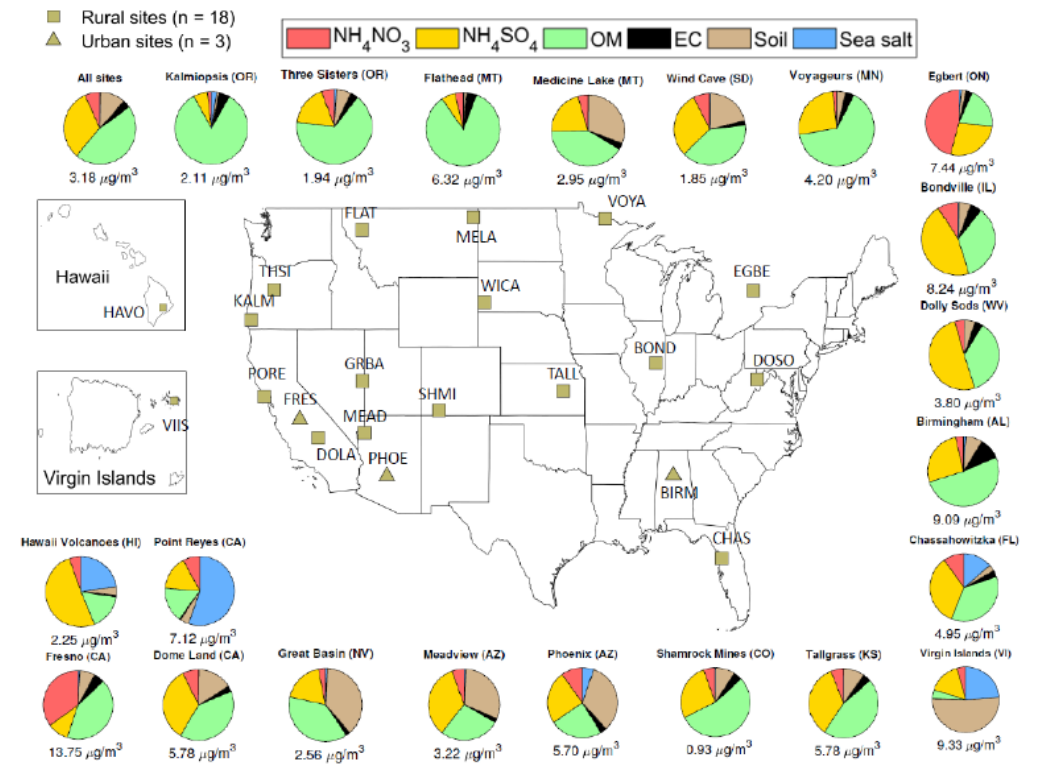
Debus, Takahama et al., *Appl. Spectroscopy*, 2018

# Example demonstration in IMRPOVE network, USA

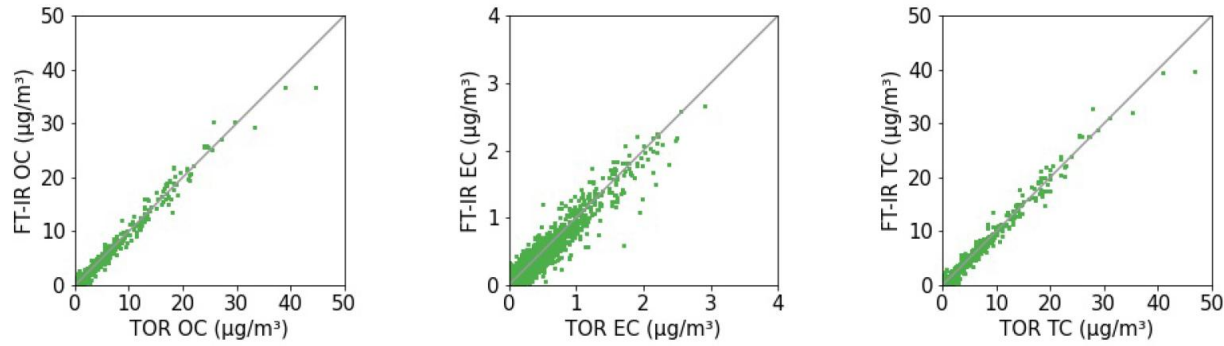
## Interagency Monitoring of Protected Visual Environments



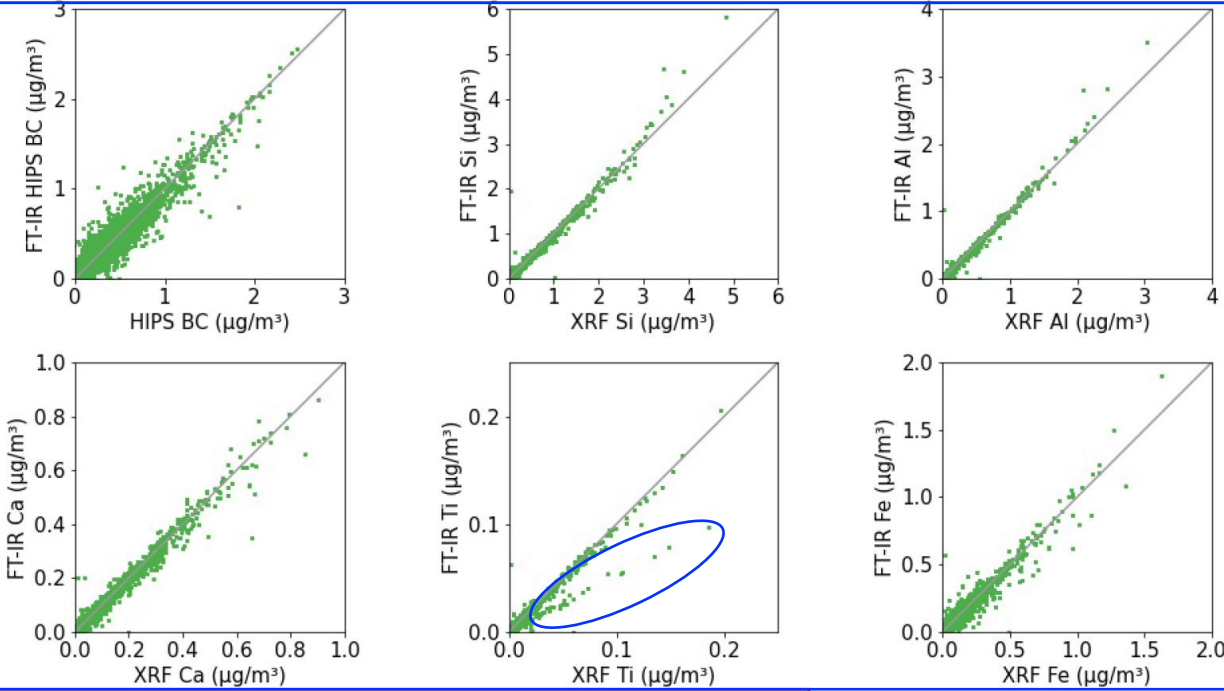
IMPROVE network, 161 sites



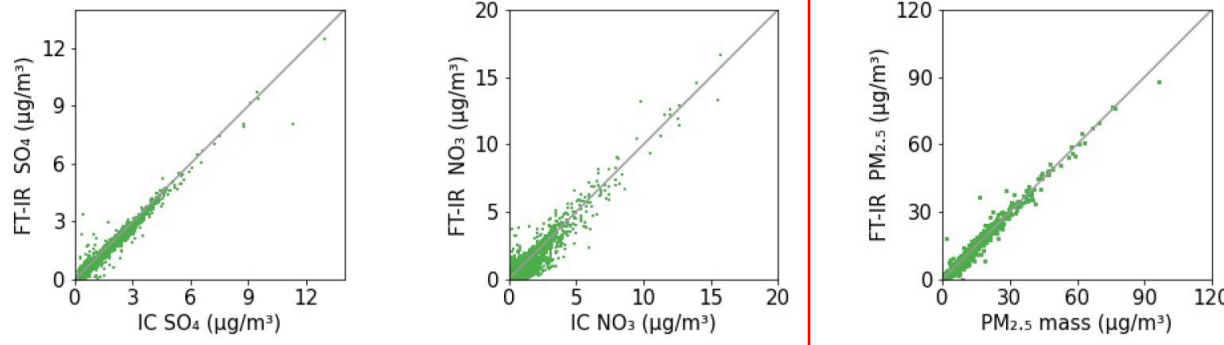
21 sites selected based on abundance of spectral types



carbon



metals



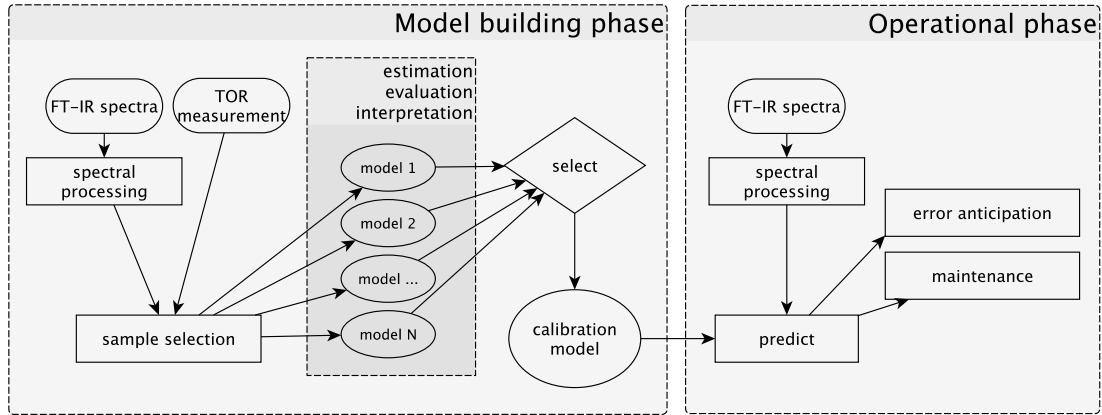
inorganic salts  
and PM<sub>2.5</sub>

Predictions for ~61,500 samples from 2015-2017

Prediction accuracy compared against collocated precision of reference

Error for Ti in Sycamore Canyon (AZ)

# Network implementation



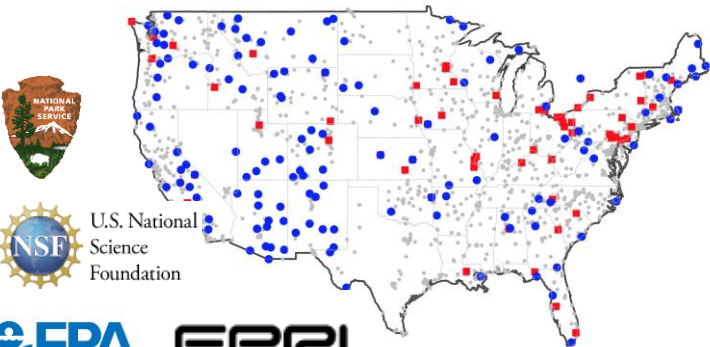
## Quantification of major species:

- Organic and elemental carbon
- Organic matter
- Inorganic salts
- Mineral dust

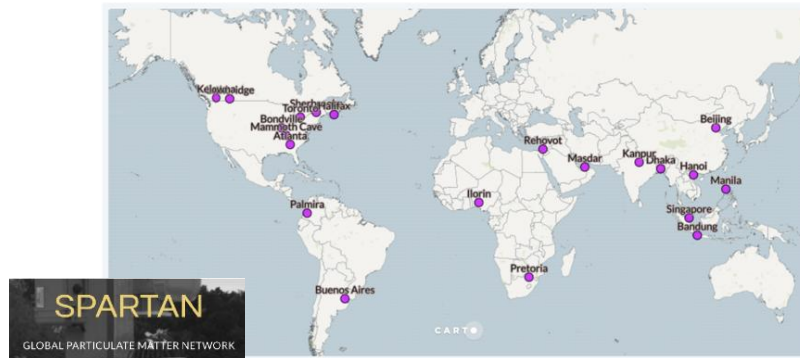
~200,000 samples

over 8 years across 5 separate monitoring networks

Takahama et al., *Atmos. Meas. Tech.*, 2019  
 Debus et al., *Atmos. Meas. Tech.*, 2022



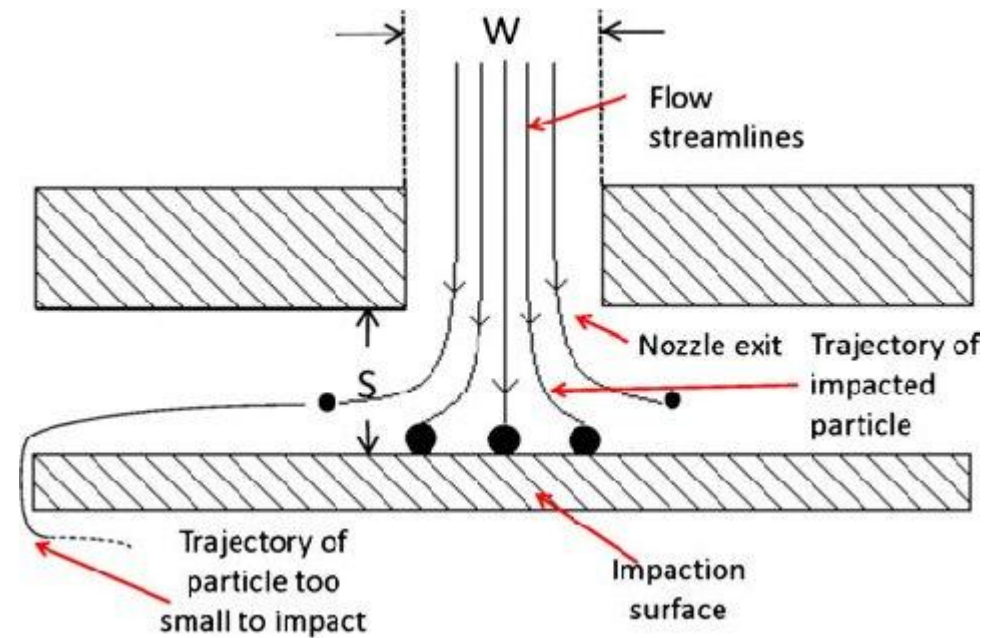
U.S. National Science Foundation



Toward an automated infrared monitor

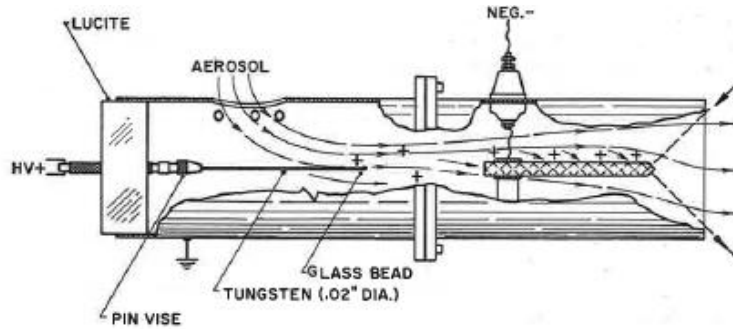
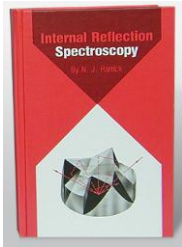
# Methods for particle collection

- Passive sedimentation
- Filtration
- Impaction
- Electrostatic deposition
- Thermophoresis

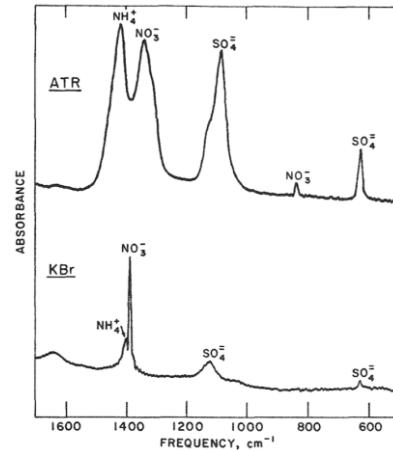
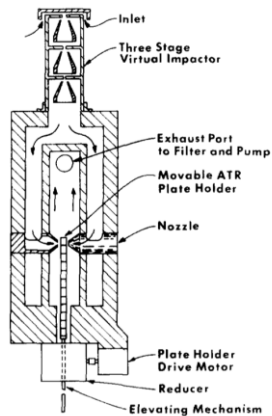


# Past designs proposed

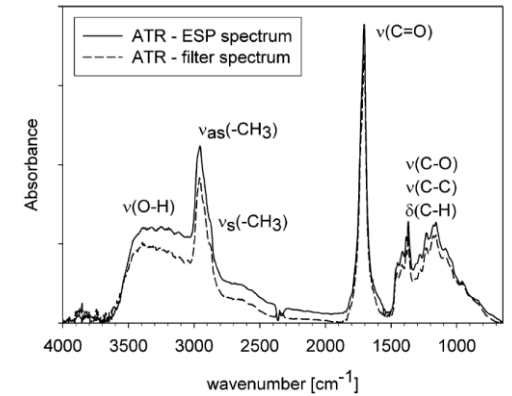
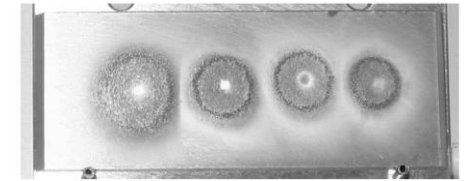
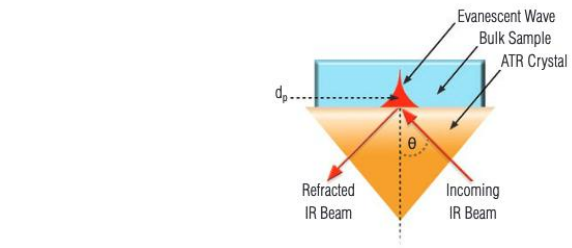
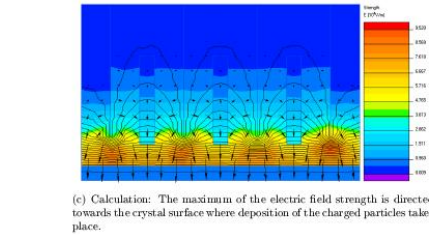
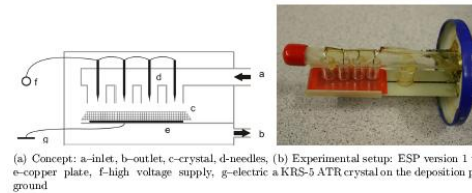
Harrick 1979  
(1<sup>st</sup> printing 1967)



Johnson 1981  
Argonne National Lab

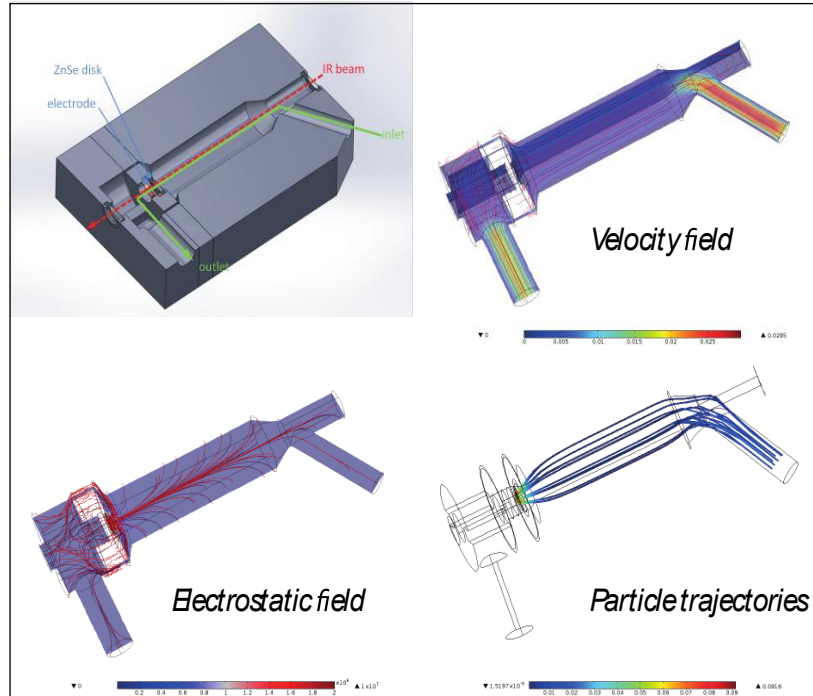


Ofner et al. 2008  
Tech. Univ. Vienna



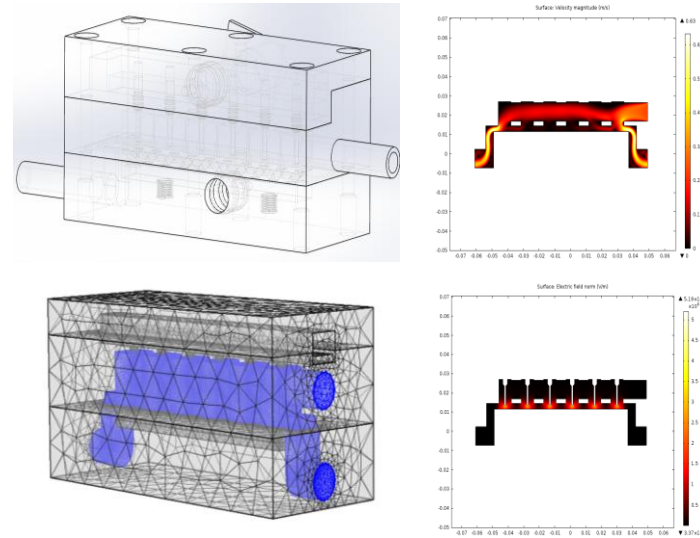
# Evolution in design at EPFL

2012-2013

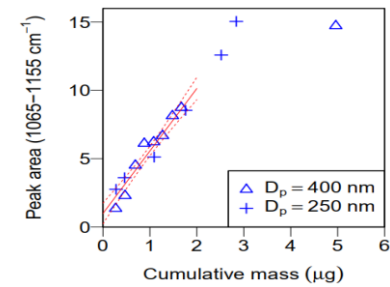


Florian Breider

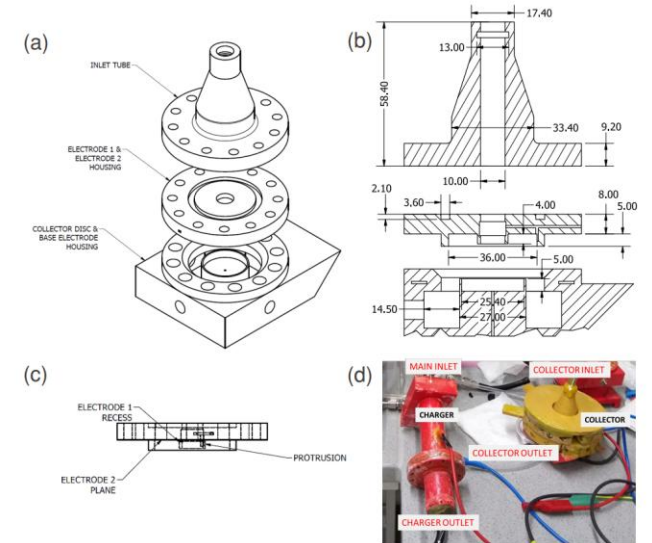
2014-2017



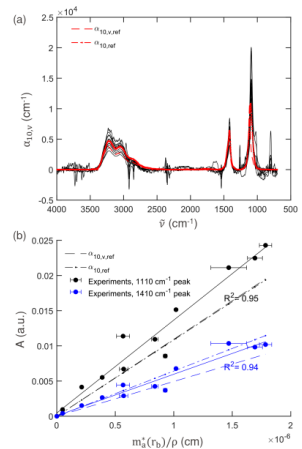
Rob Modini  
Christophe Delval



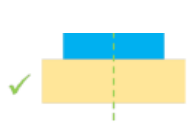
2017-2019



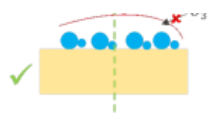
Nikunj Dudani



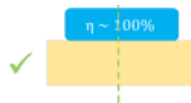
# Core innovation in particle collection



Uniform deposition



Minimal chemical modification



High collection efficiency



Low particle size dependence



High throughput

$$r_f/R_c = \Omega \left( \frac{r_i^*}{r_{lim}^*} \right) \sqrt{r_{geo}^{\dagger 2} + 3\alpha\beta \left( \frac{2 - \Omega^2 r_i^{*2}}{2 - r_{lim}^{*2}} \right)}$$

$$\Omega = \frac{r_0^*}{r_i^*} = f \left( r_i^*, \frac{H}{R}, \frac{R}{R_c}, \alpha, \beta \right); r_{geo}^{\dagger} = \left( \frac{r_{lim}^* R}{R_c} \right); \alpha = \frac{Q_a \mu}{e E_0 R_c}; \beta = \frac{D_p}{n C_c R_c}; r_0^* = \frac{r_0}{R}; r_{lim}^* = \frac{r_{i,max}}{R}$$

$$0 \leq r_i \leq r_{lim}^*; 0 \leq \Omega \leq 1$$

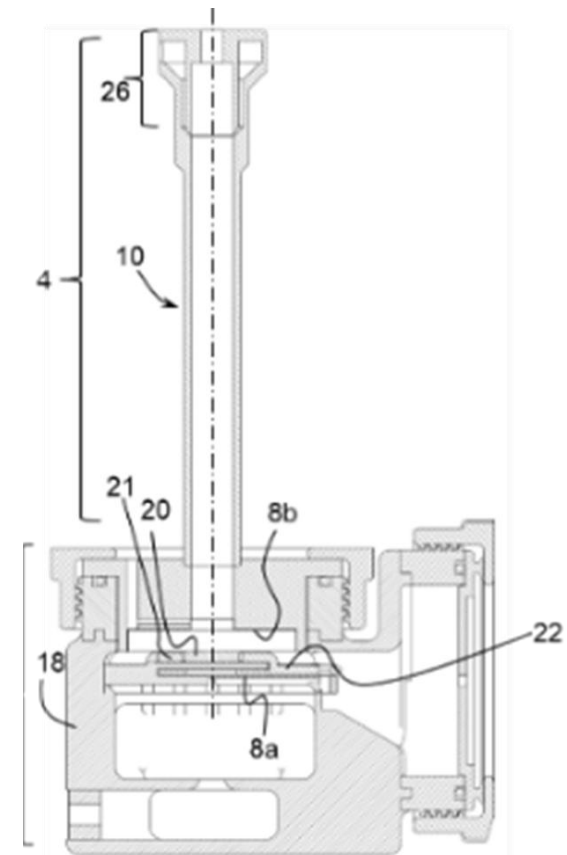
$$\Omega^3 - \frac{3}{r_i^{*2}} \left( 1 + \frac{v_{elec,r}}{2v_{in}} \right) \Omega - \left\{ 1 - \frac{3}{r_i^{*2}} \left( 1 + \frac{v_{elec,r}}{2v_{in}} \right) + \frac{3}{r_i^{*3}} \left( \frac{v_{elec,r}}{2v_{in}} \right) \right\} = 0$$

where  $v_{in}/v_{elec} = \frac{1}{E_{corr}} \frac{3\alpha\beta}{r_{lim}^{*2} (2 - r_{lim}^{*2})} \left( \frac{R}{R_c} \right)^{-2}; E_{corr} = f(H/R)$

Geometric variables	Operating variables	Inlet variables	Performance variables
$R_c$ : Collection disc radius $R$ : Inlet radius $H$ : Electrode separation distance	$Q_a$ : Aerosol flow rate $E$ : Electric field strength $V_0$ : Voltage difference between $z=0$ and $z=H$	$D_p$ : Particle diameter $n$ : no. of elementary charges on the particle $r_{lim}^*$ : Sheath position $r_i^*$ : Inlet position	$\frac{r_f}{R_c}$ : Dimensionless final position of deposition

Dudani, PhD thesis, 2021

Dudani and Takahama (US patent) filed 2020; granted 2024

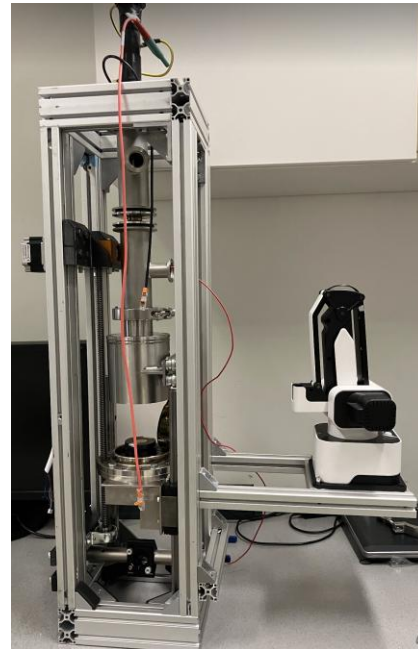


# Toward an automated instrument

Prototype collector  
3-D printed  
2019-2021

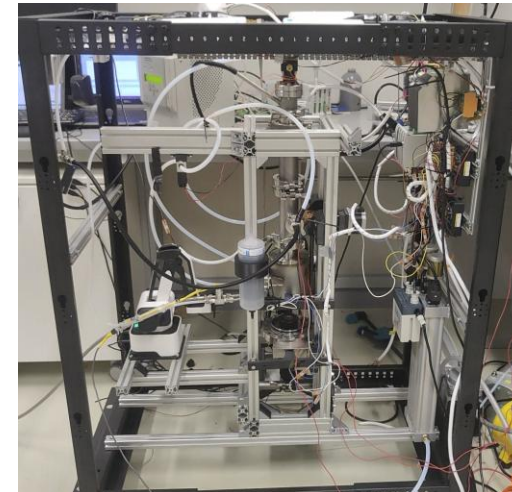


Sample collector  
machine fabrication  
2023

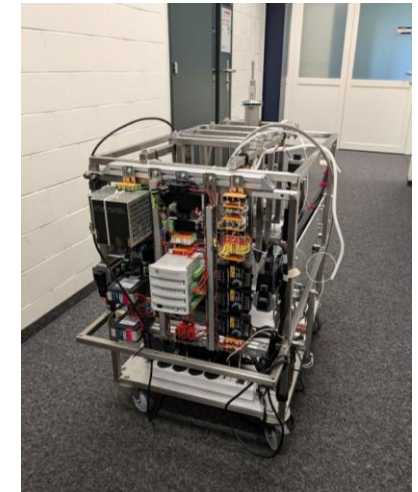


Fully-integrated  
online monitor  
2023-2024

*Prototype v1*



*Prototype v2*



Aerospec



**Nikunj Dudani**  
CEO, Co-founder



**Satoshi Takahama**  
Scientific advisor, Co-Founder



**Andrea Baccarini**  
CTO



**Arthur Blase**  
Product engineer, Business development



**Kamila Babayeva**  
Programming guru

Thanks for your attention!